Dynamical mechanisms of accretion in galactic nuclei.

Study of stability, accretion, and tidal disruption near supermassive black holes with advanced parallel computer technologies.

VolkswagenStiftung

12 referred + 4 in progress (2020 – 2021):

MNRAS – 7; A&A – 4; ApJ – 1

~97 citations…

Dr. Sci. Peter Berczik
Dr. Alexander Veles
Dr. Marina Ishchenko
Margarita Sobolenko
Daniel Ivanov

MAO, National Academy of Sciences of Ukraine, Kiev

2021 September 6-8, VW meeting.

BH's in galaxies (MW - Sgr A*)

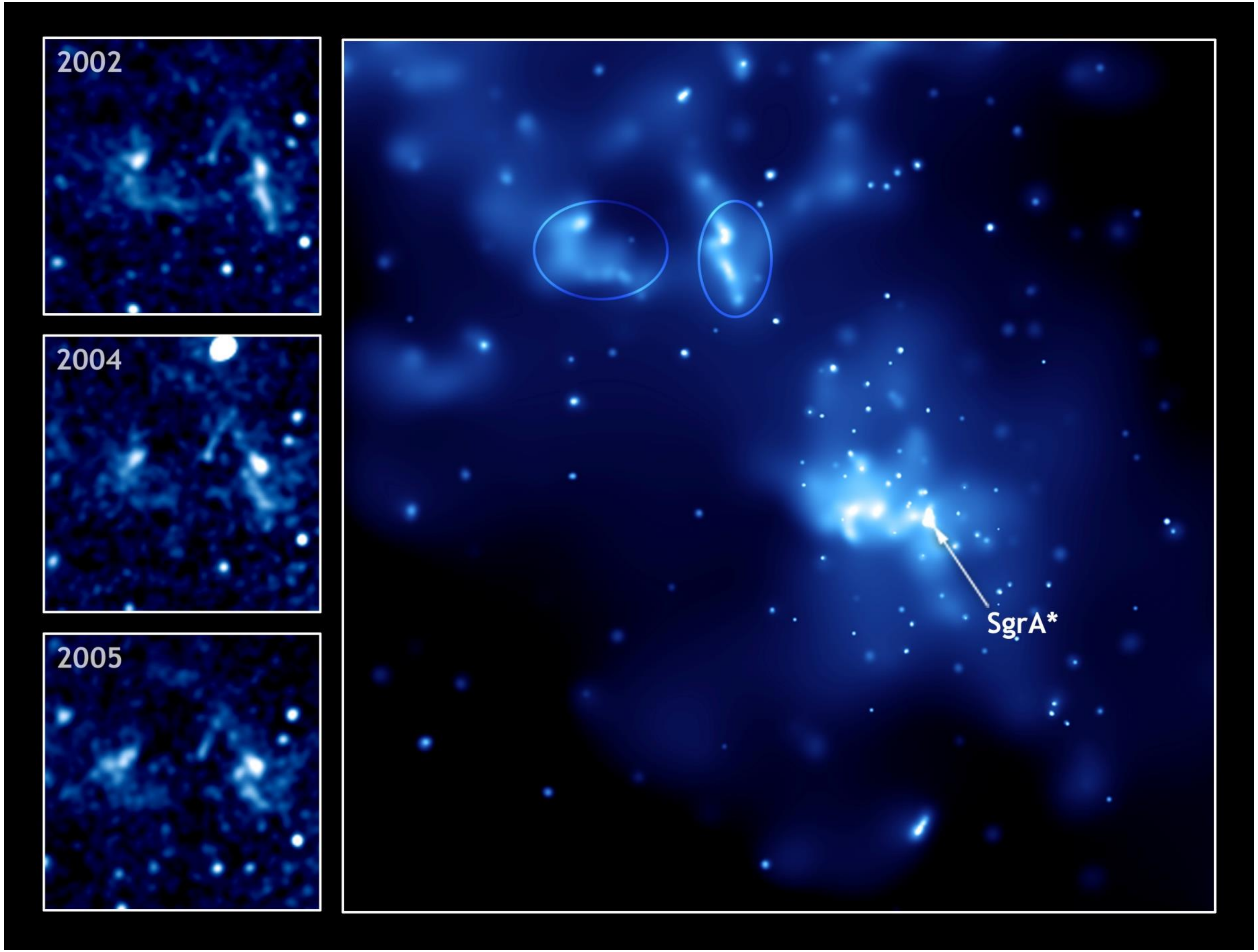

BH's in galaxies (MW - Sgr A*)

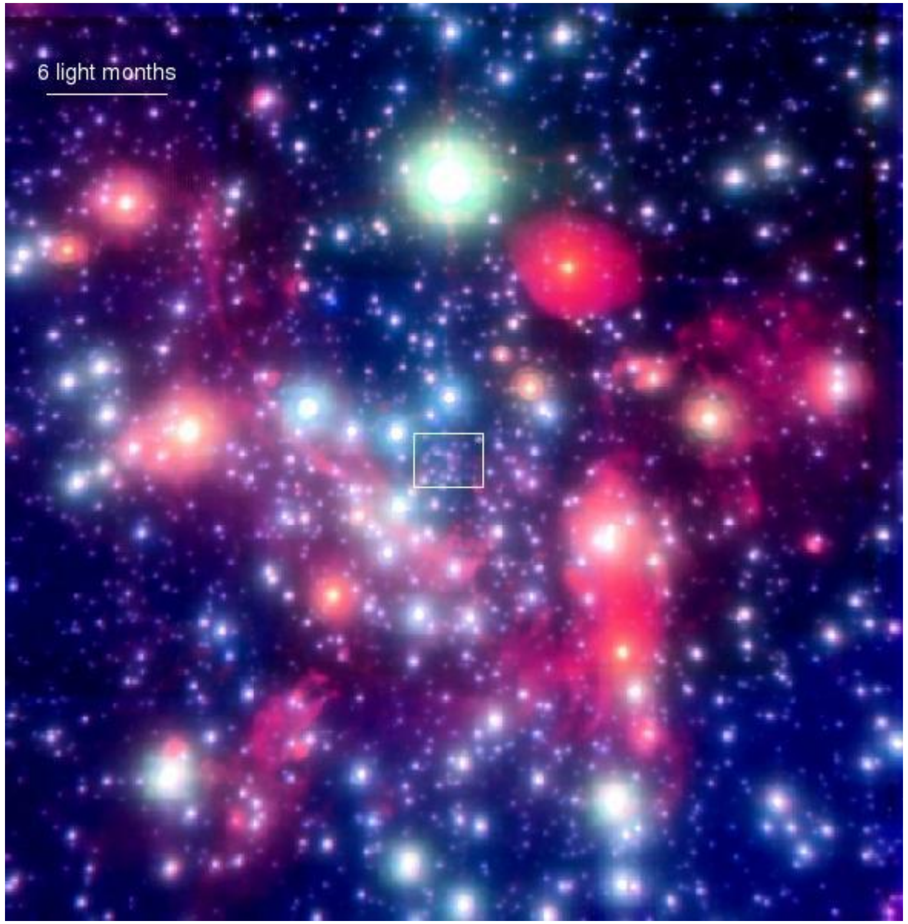

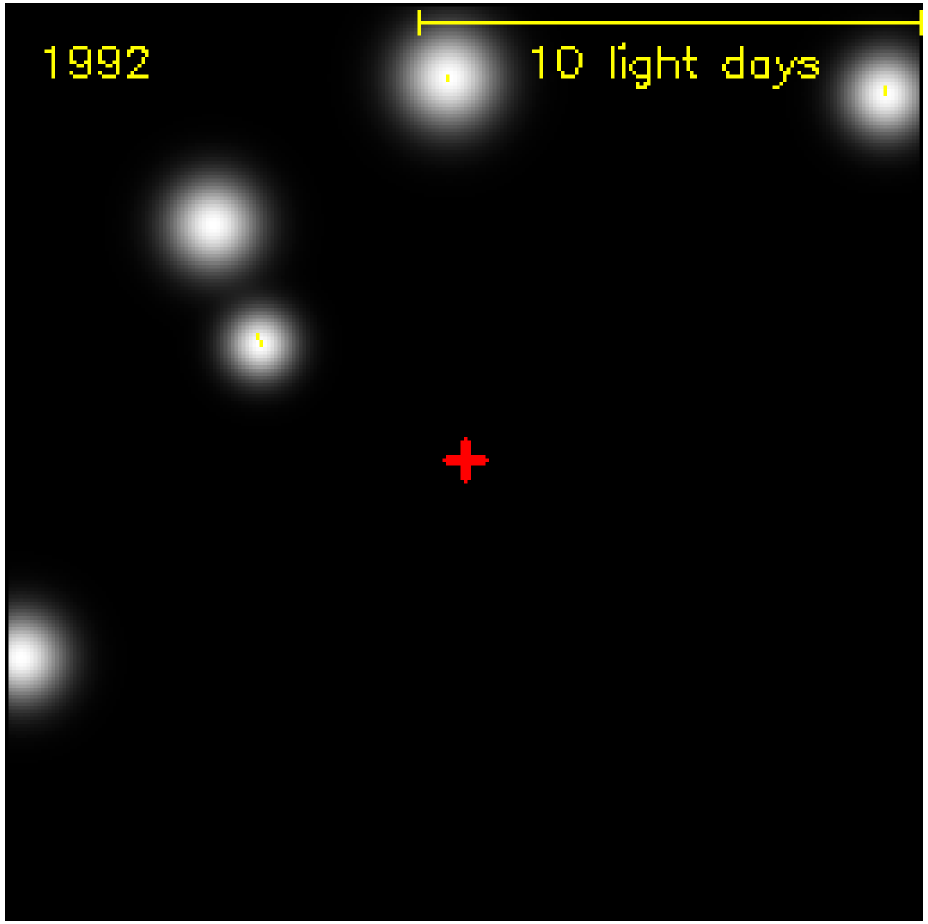

BH's in galaxies

$$M \propto \sigma^{\alpha}.$$
$$\alpha = 4.2 \pm 0.4.$$

(Faber et al. 1987)

$$M \sim L^{5/4} \quad L \sim \sigma^4$$
$$M \sim \sigma^5$$

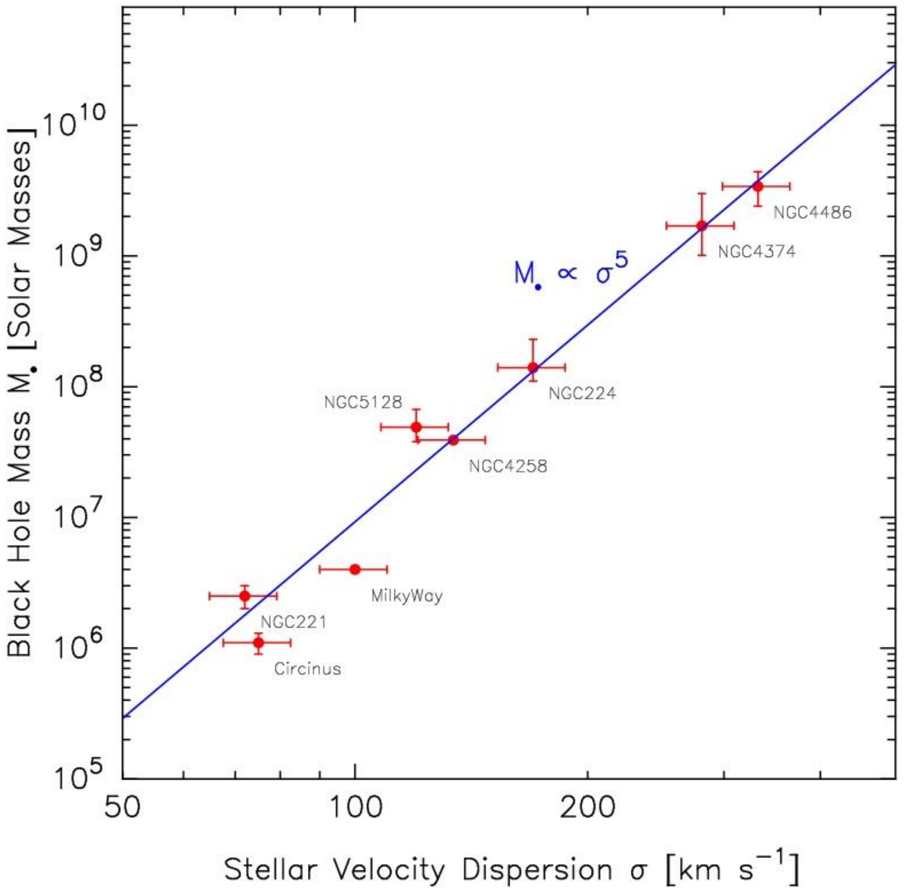

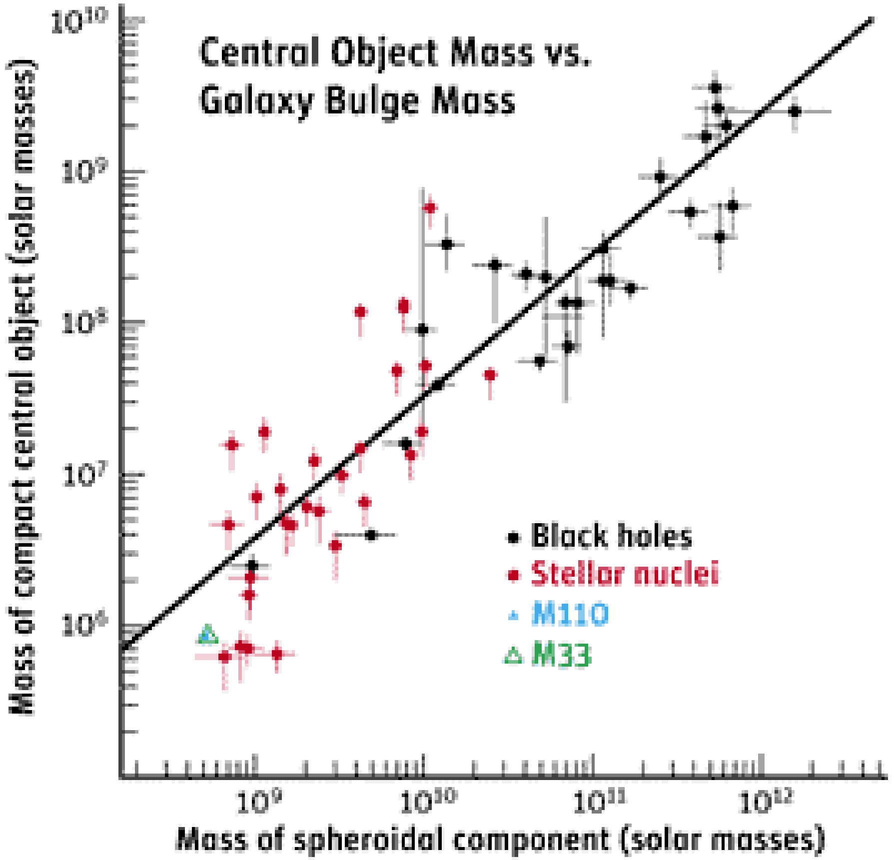

BH's in galaxies

THE ASTROPHYSICAL JOURNAL, 698:198–221, 2009 June 10
doi:10.1088/0004-637X/698/1/198

THE M–σ AND M–L RELATIONS IN GALACTIC BULGES, AND DETERMINATIONS OF THEIR INTRINSIC SCATTER

KAYHAN GÜLTEKIN[1], DOUGLAS O. RICHSTONE[1], KARL GEBHARDT[2], TOD R. LAUER[3], SCOTT TREMAINE[4], M. C. ALLER[5], RALF BENDER[6], ALAN DRESSLER[7], S. M. FABER[8], ALEXEI V. FILIPPENKO[9], RICHARD GREEN[10], LUIS C. HO[7], JOHN KORMENDY[2], JOHN MAGORRIAN[11], JASON PINKNEY[12], AND CHRISTOS SIOPIS[13]

$$\log(M/M_\odot) = 8.12 \pm 0.08 \;+\; (4.24 \pm 0.41)\log(\sigma/200\ km\ s^{-1})$$

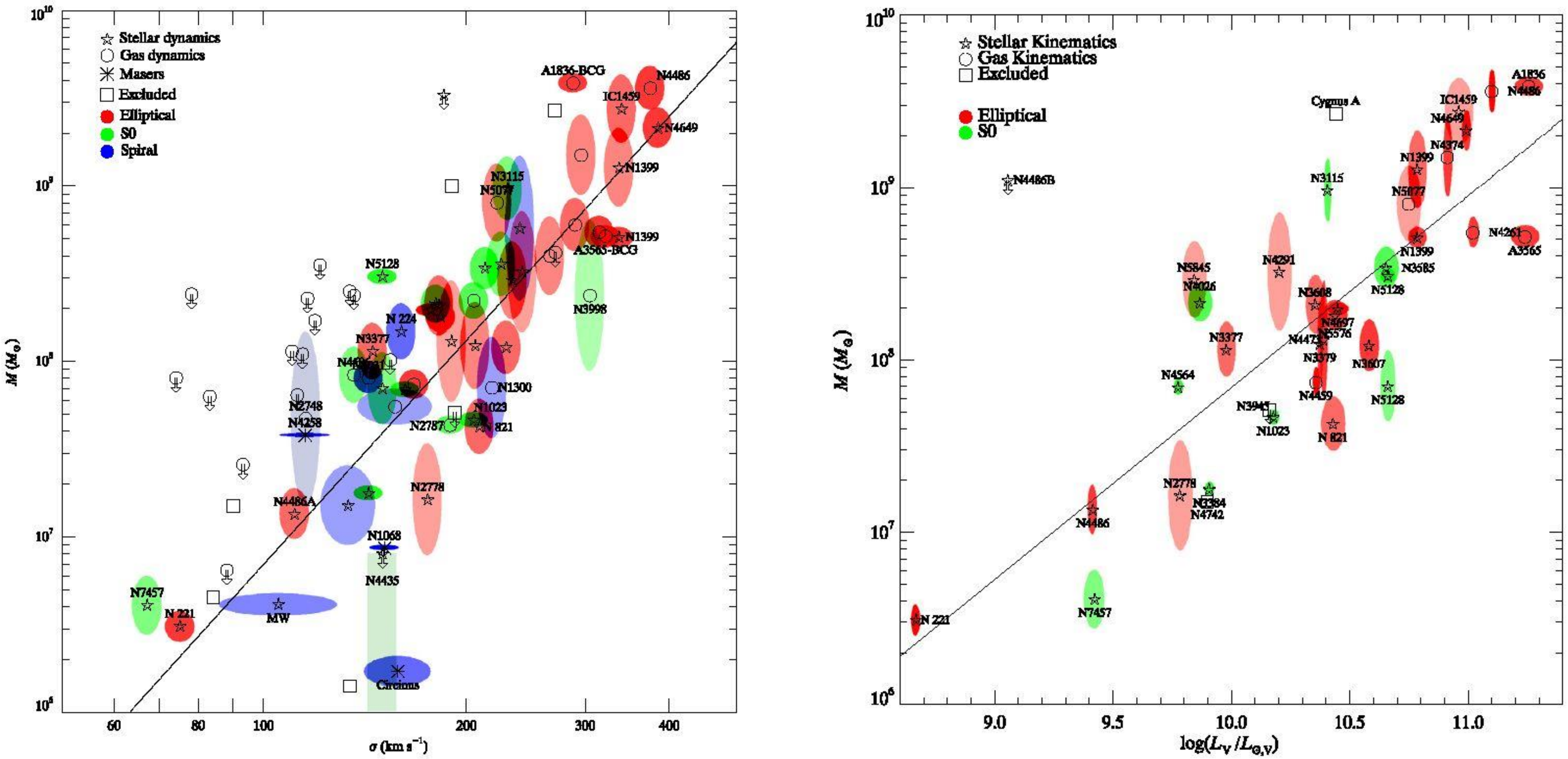

Galaxy Collisions

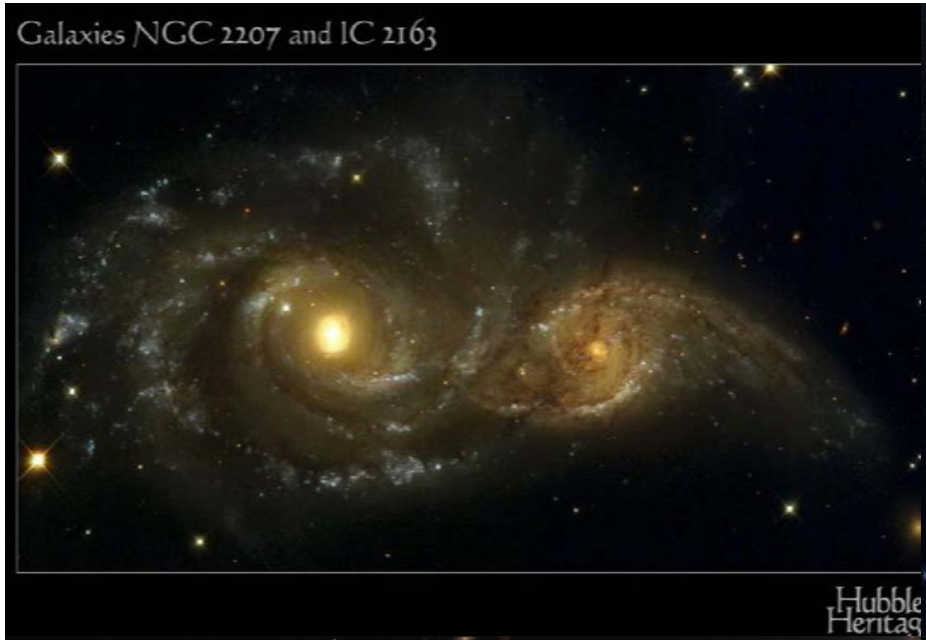

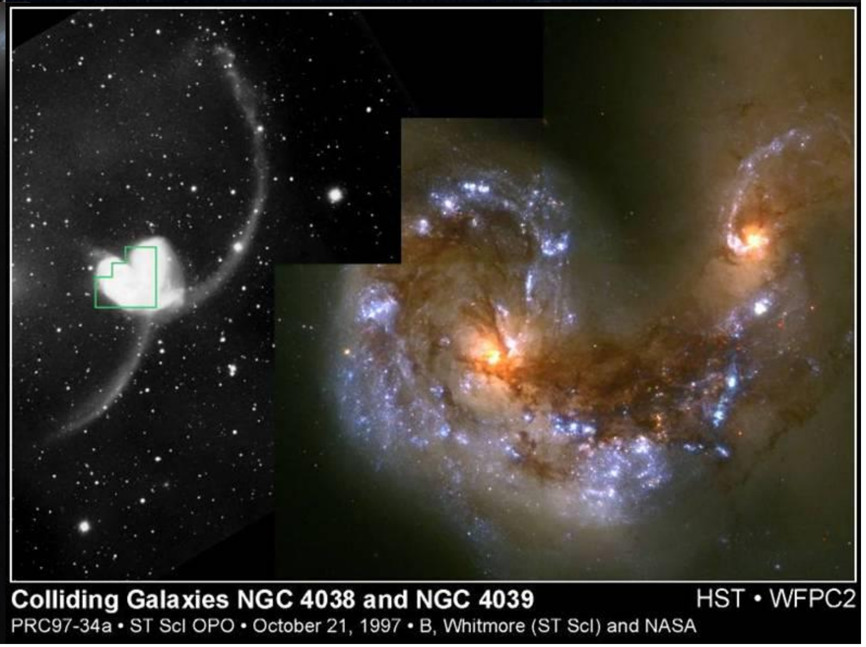

Galaxy Collisions ≈ BH's collisions

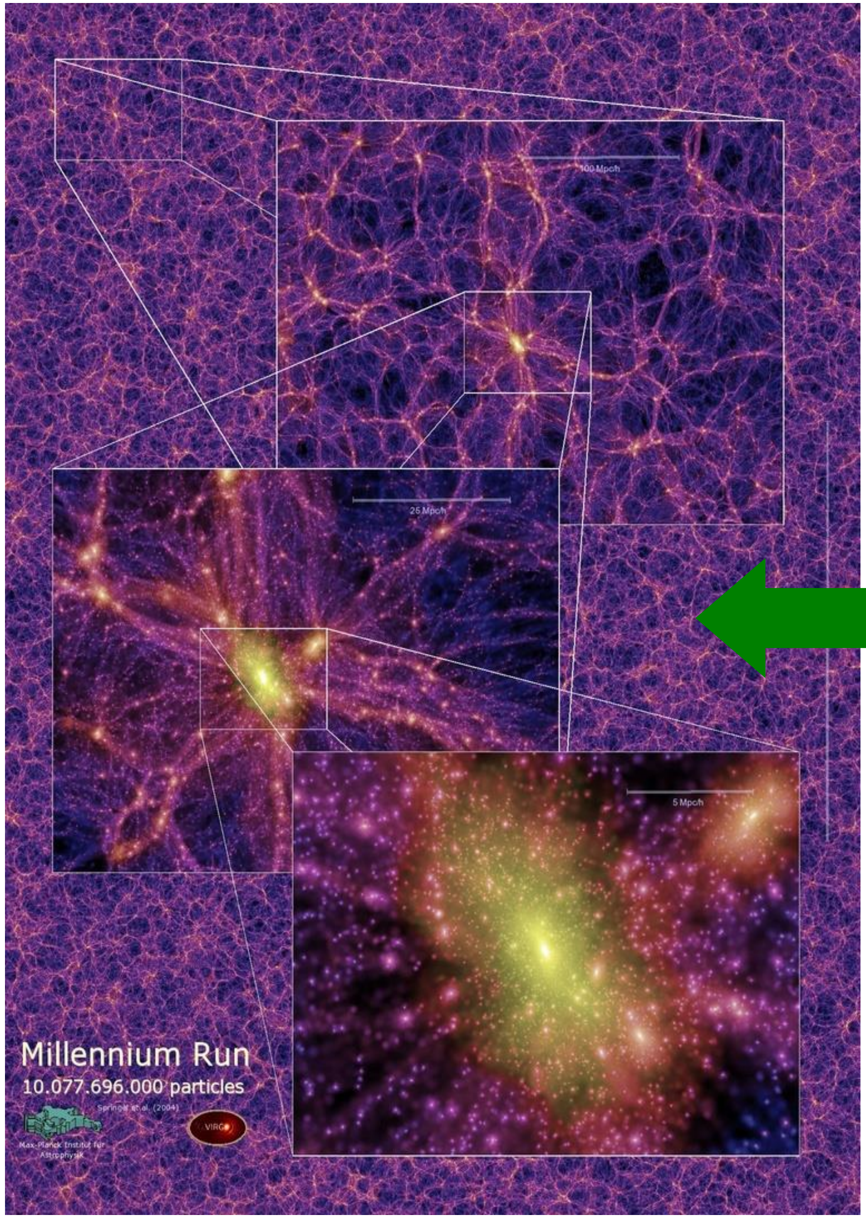

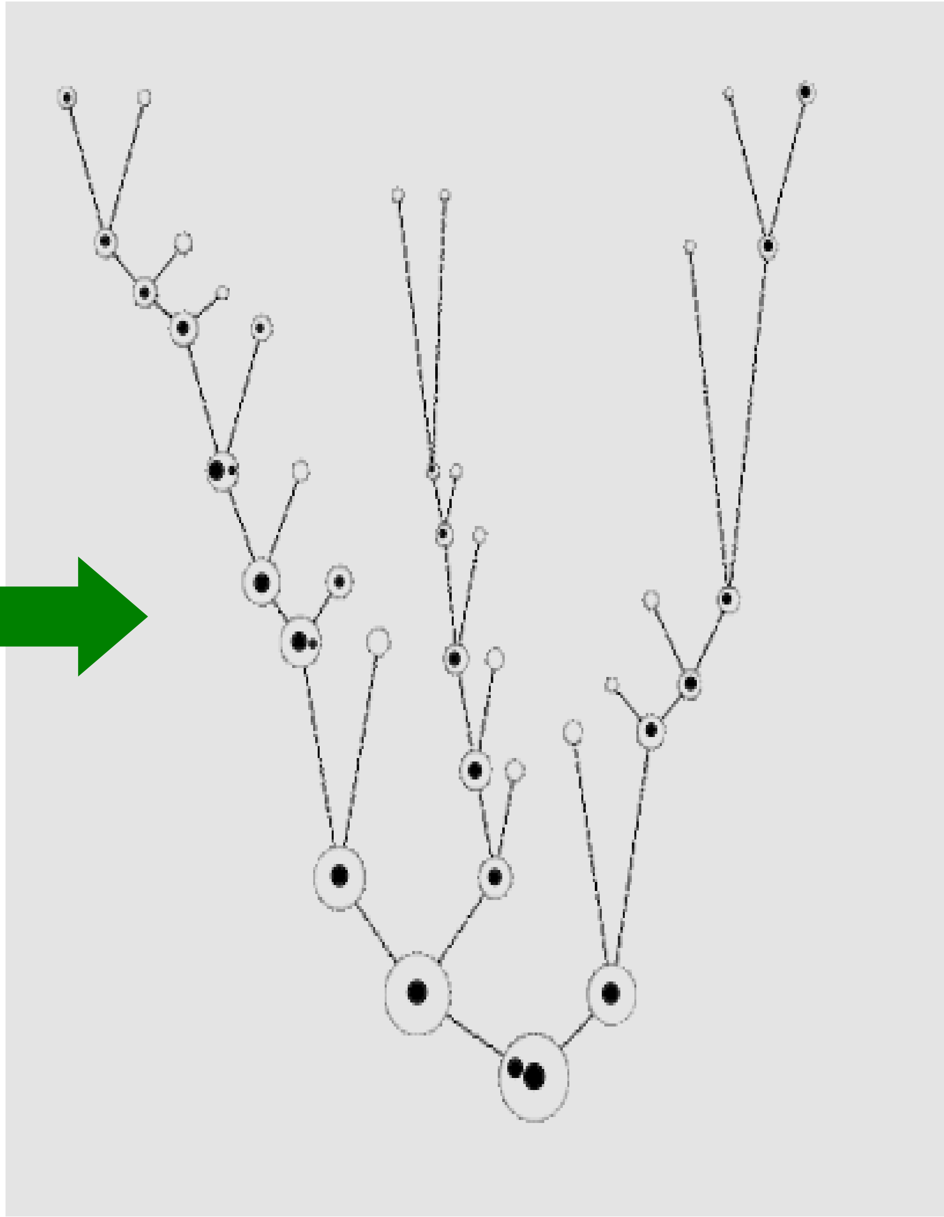

Galaxy Collisions ≈ BH's collisions

Multiple Massive Black Holes
NGC6240
strong ongoing merger…
Komossa et al. 2002

Two AGN in each of Nuclei separation
~1kpc Chandra X-Ray

M82: The bright spots in the center are supernova remnants and X-ray binaries. The luminosity of the X-ray binaries suggests that most contain a black hole. A close encounter with a large galaxy, M81, in the last 100 Myr is thought to be the cause of the starburst activity. Ebisuzaki et al. 2002

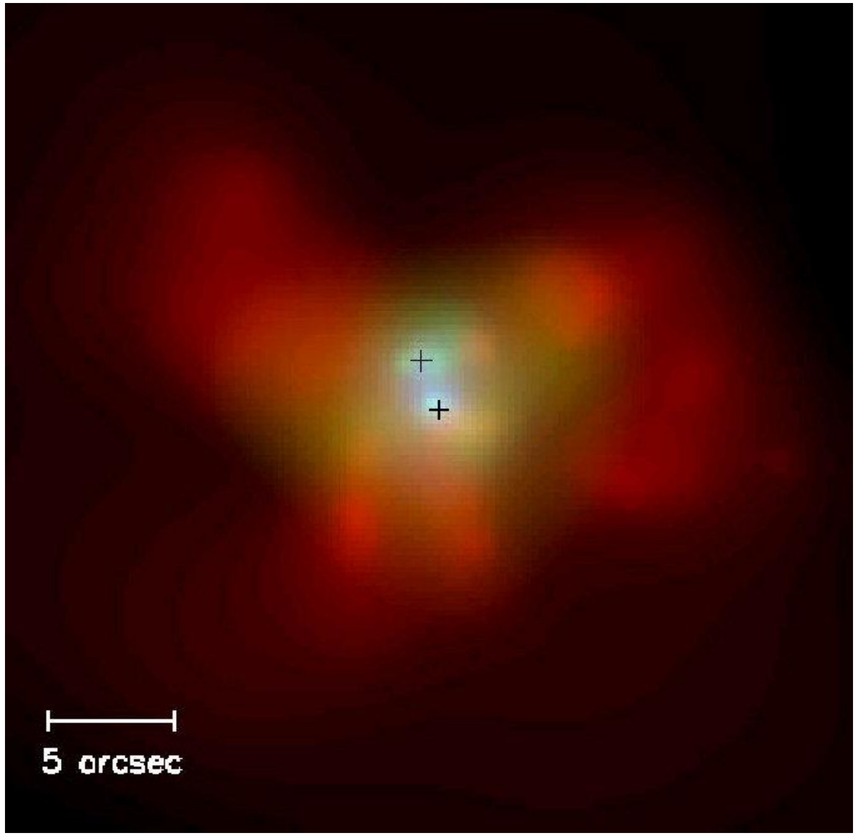

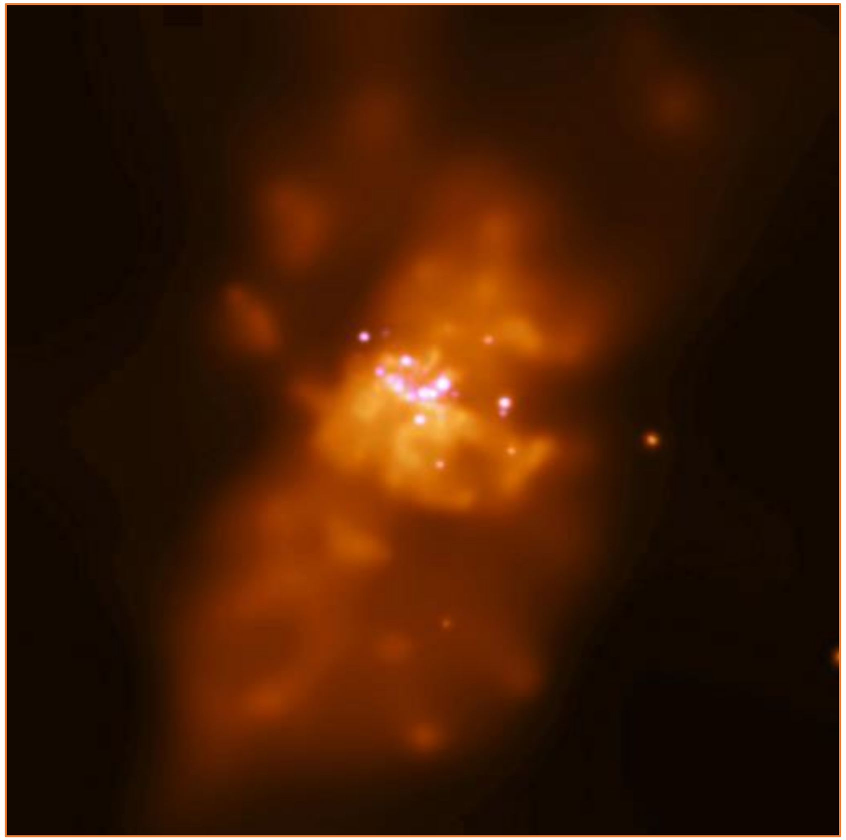

Galaxy Collisions ≈ BH's collisions

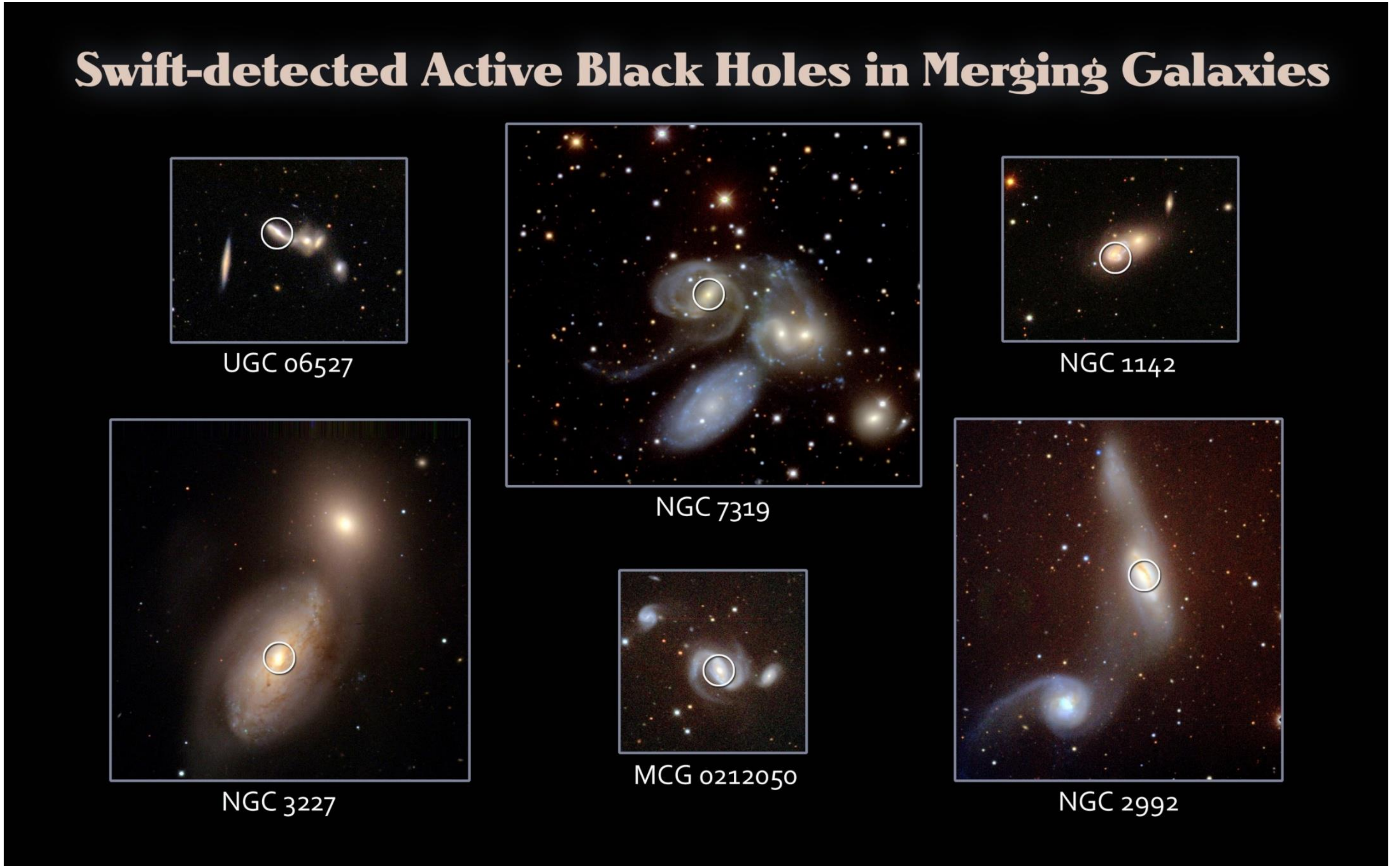

Double & Triple SMBH evolution in galaxy centers. New hybrid code approaches and performance tests.

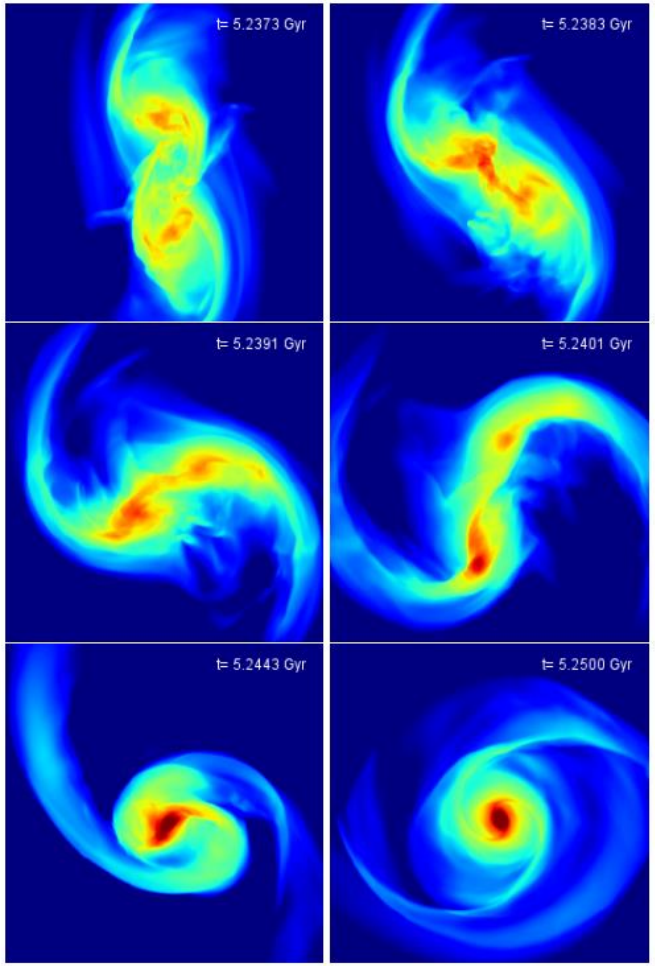

Figure 1. Mass-weighted gas density maps during last pericenter and final merger. The line-of-sight is perpendicular to the orbital plane and the maps are 1.8 kpc wide. While fairly symmetric before the pericenter (top left), the density distribution becomes clearly asymmetric after the pericenter (middle). After the final merger, a thick $\sim 10^9$ $M_\odot$ gaseous nuclear disk is formed (bottom), in which the two SMBHs start orbiting.

1:10 minor merger

Two SMBH's ~10^6 Mo

High accuracy direct summation: ~3M Particles!

First time reach the < 1 mpc separation of BBH from initial ~1 kpc scale

<u>Full up to 3.5 PN accurate BBH dynamics!</u>

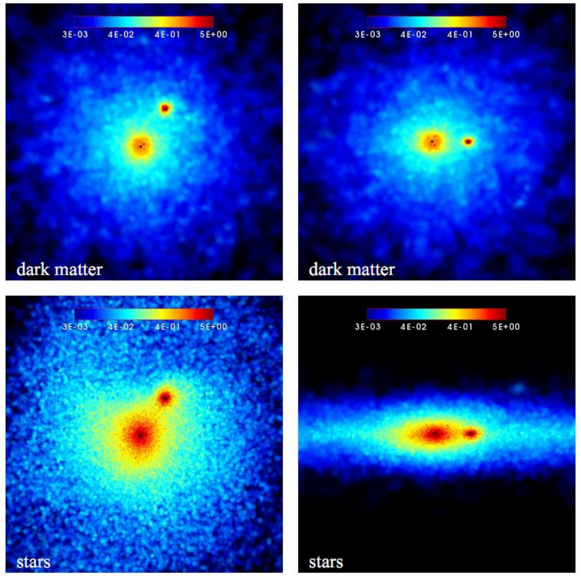

FIG. 1.— Density distribution of the dark matter (top panels) and stellar component (bottom panels) in the $x-y$ (left column) and $y-z$ (right column) planes. The two high density regions are clearly visible around the two SMBHs (black dots) in the center. The size of each box is 4 kpc.

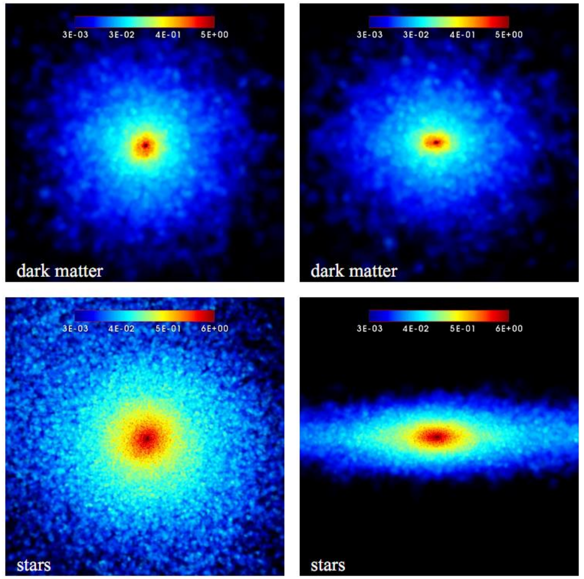

FIG. 3.— Same as in Figure 1 but at $T = 40$ Myr. Both SMBHs are embedded in a single cusp.

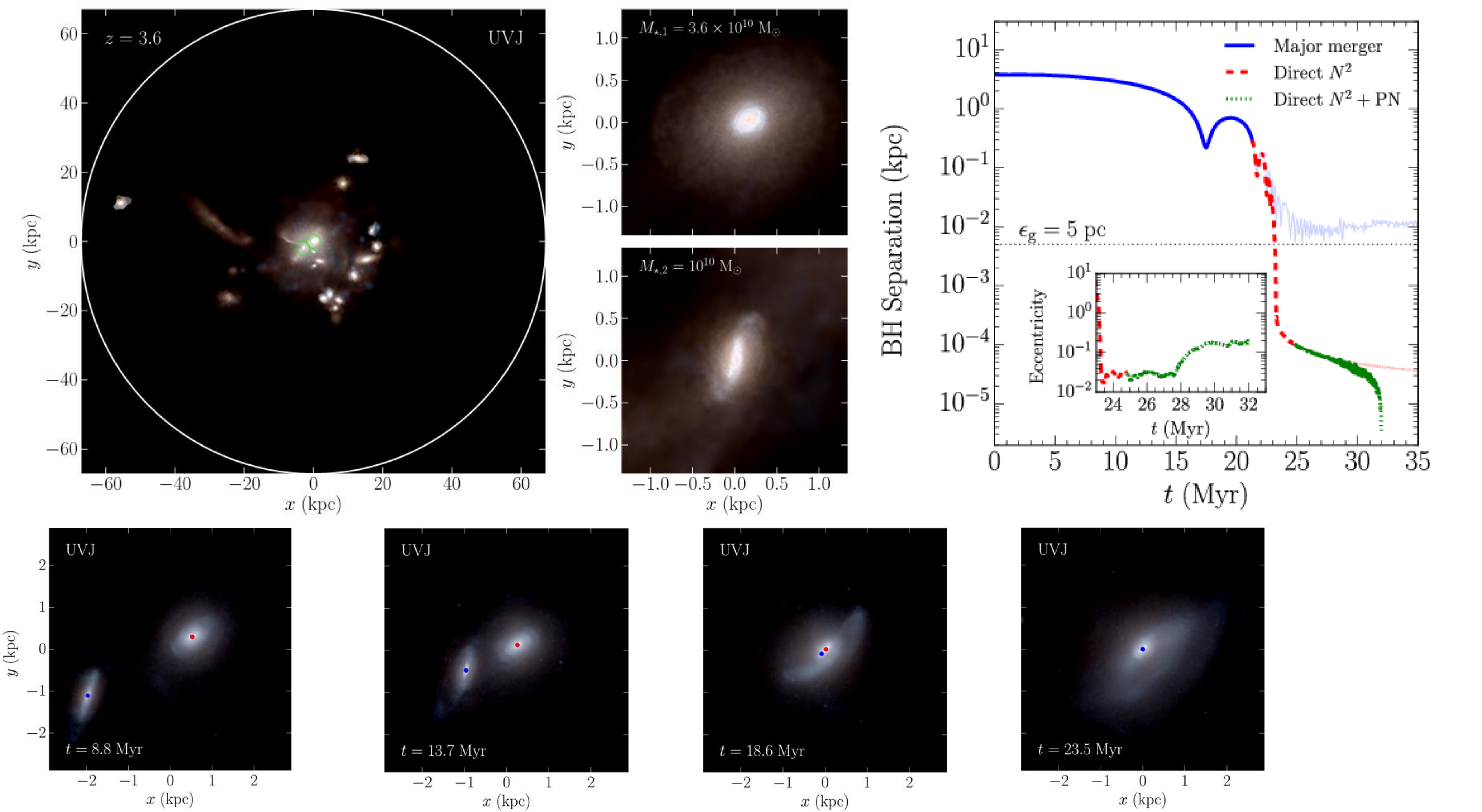

$z = 3.6$
UVJ
$M_{\star,1} = 3.6 \times 10^{10}$ M$_\odot$
$M_{\star,2} = 10^{10}$ M$_\odot$
Major merger
Direct N^2
Direct N^2 + PN
$\epsilon_g = 5$ pc
BH Separation (kpc)
Eccentricity
t (Myr)
x (kpc)
y (kpc)
$t = 8.8$ Myr
$t = 13.7$ Myr
$t = 18.6$ Myr
$t = 23.5$ Myr

Our φGRAPE/GPU N-body code

Harfst et al, NewA, 12, 357 (2007) [astro-ph/0608125]

Hierarchical Individual Block Time Steps

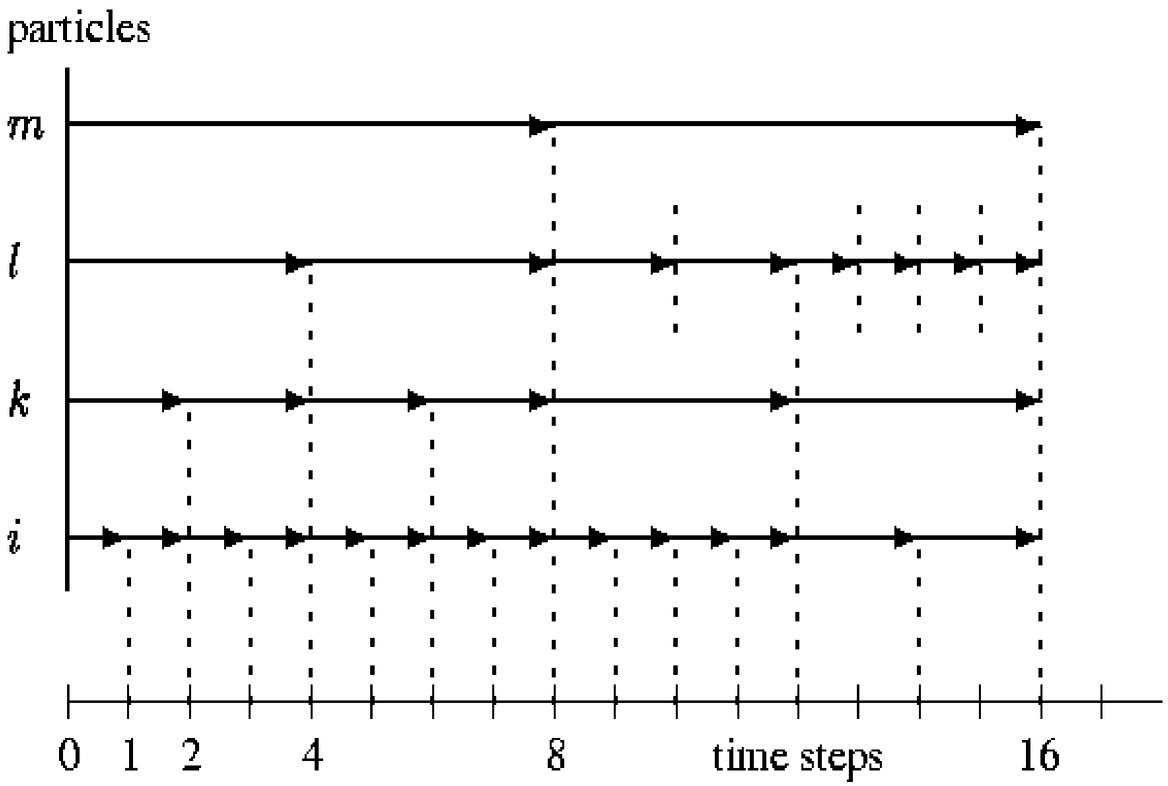

$$\Delta t = \sqrt{\eta \frac{|\vec{a}||\vec{a}^{(2)}| + |\dot{\vec{a}}|^2}{|\dot{\vec{a}}||\vec{a}^{(3)}| + |\vec{a}^{(2)}|^2}} \; .$$

4th order Hermite scheme

$$\frac{d^2\vec{r}_i}{dt^2} = \vec{a}_i$$

ftp://ftp.mao.kiev.ua/pub/berczik/phi-GRAPE/

Our φGRAPE/GPU N-body code

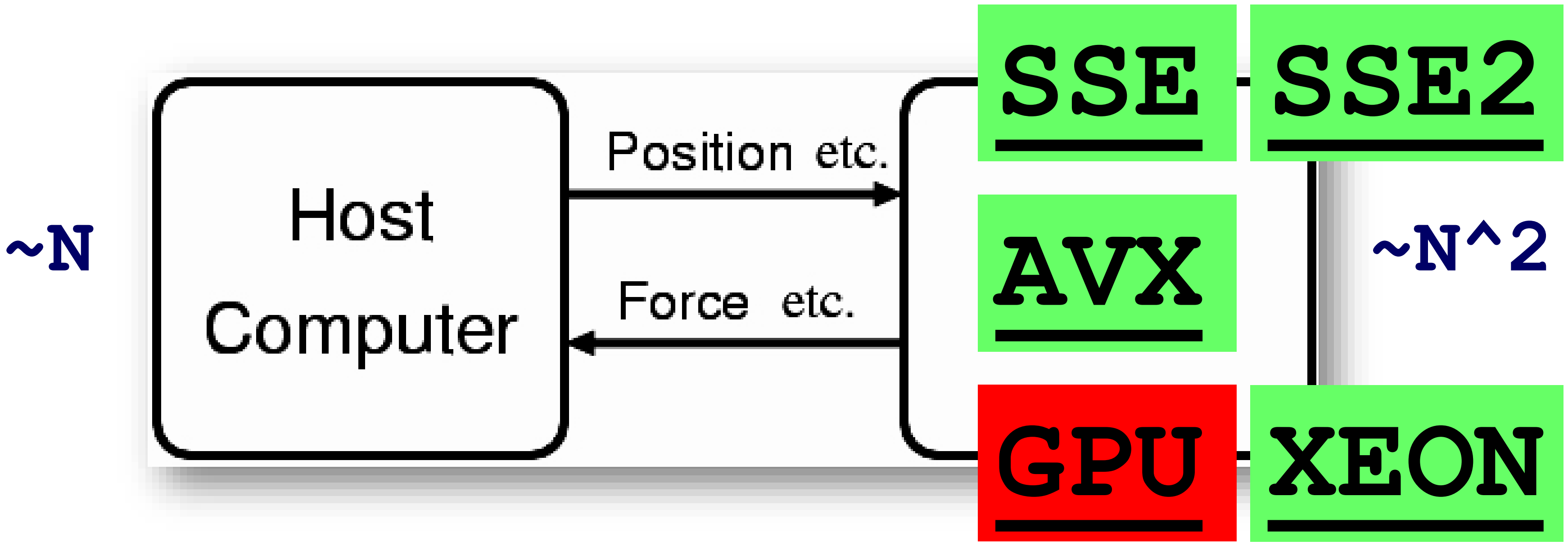

$$\vec{a}_i = \sum_{j=1;\, j\neq i}^{N} \vec{f}_{ij} \qquad \vec{f}_{ij} = -\frac{G \cdot m_j}{(r_{ij}^2 + \varepsilon^2)^{3/2}} \vec{r}_{ij}$$

ftp://ftp.mao.kiev.ua/pub/berczik/phi-GRAPE/

Our φGRAPE/GPU N-body code

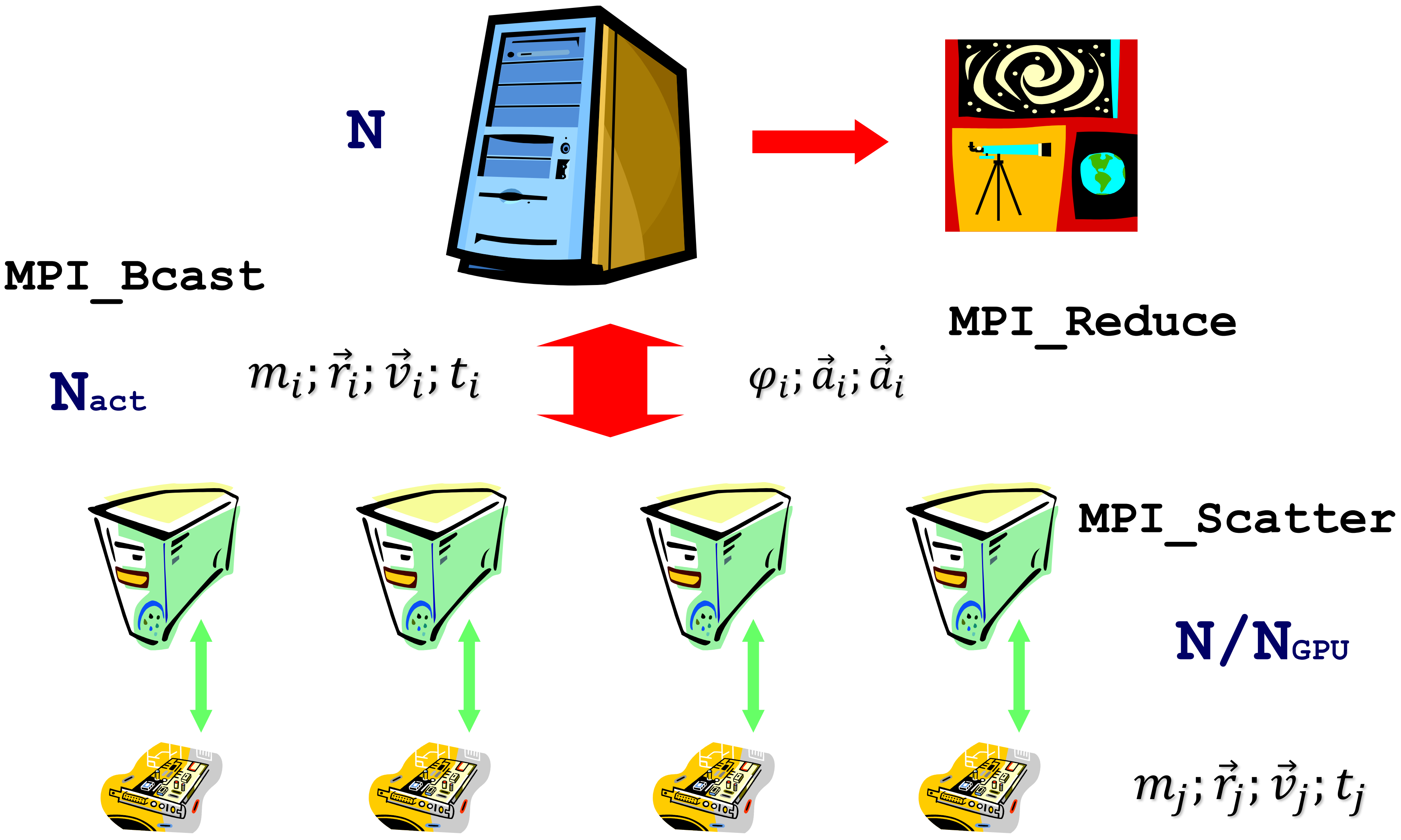

Our φGRAPE/GPU N-body code

$$i, j - particle$$

Some communication scheme...

$$N_{loc} = \frac{N}{N_{proc}}$$

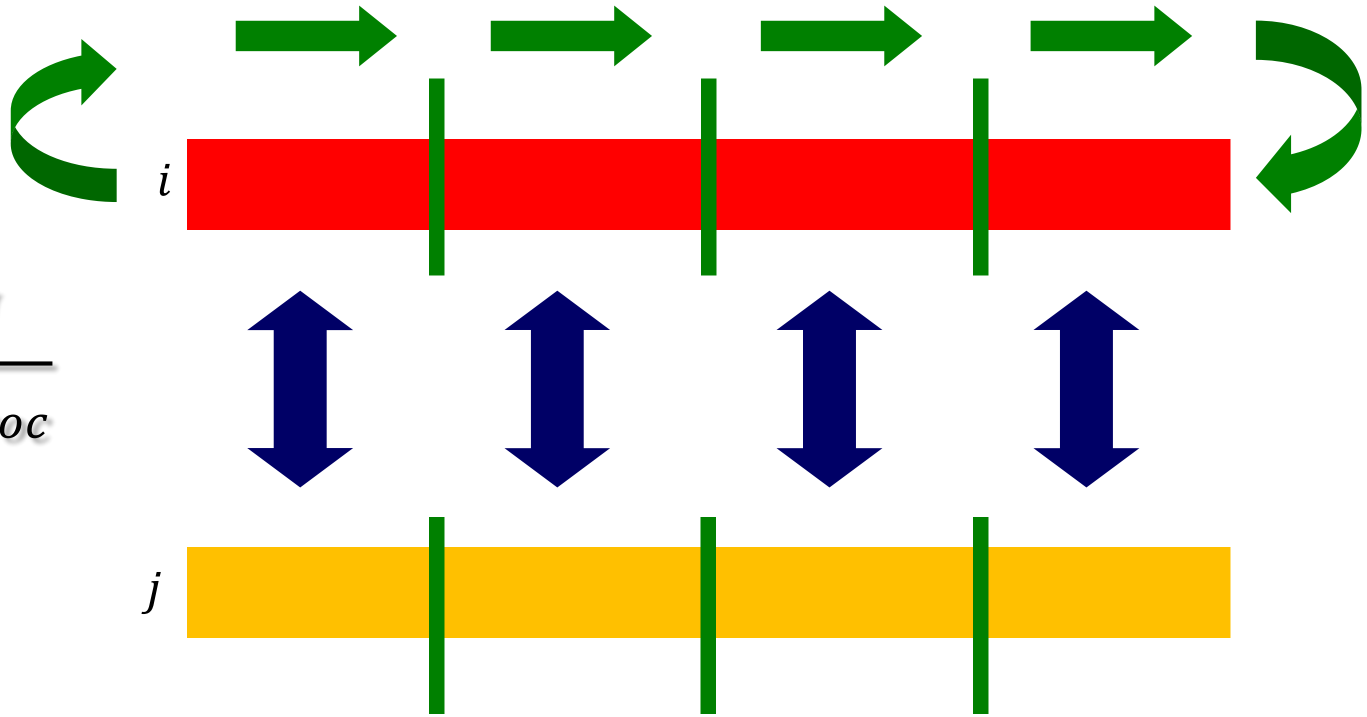

Our φGRAPE/GPU N-body code

http://adsabs.harvard.edu/abs/2011hpc..conf....8B

• active part. scan:	$O(N_{act}\ \log(N_{act}))$	$+T_{host}$
• all part. prediction:	$O(N/N_{GPU})$	$+T_{host}$
• ‘‘j’’ part. send. to GPU:	$O(N/N_{GPU})$	$+T_{comm}$
• ‘‘i’’ part. send. to GPU:	$O(N_{act})$	$+T_{comm}$
• ‘‘force’’ determ. on GPU:	$O(N\ N_{act}/N_{GPU})$	$+T_{GPU}$
• receive the ‘‘force’’:	$O(N_{act})$	$+T_{comm}$
• MPI global comm.:	$O((\tau_{lat}+N_{act})\ \log(N_{GPU}))$	$+T_{MPI}$
• corr. for ‘‘i’’ part.:	$O(N_{act})$	$+T_{host}$

ftp://ftp.mao.kiev.ua/pub/berczik/phi-GPU/

Our φGRAPE/GPU N-body code

http://adsabs.harvard.edu/abs/2011hpc..conf....8B

$$\Delta T_{total} = \Delta T_{host} + \Delta T_{GPU} + \Delta T_{comm} + \Delta T_{MPI}$$

$$\Delta T_{MPI} \propto (\tau_{lat} + N_{act}) \cdot \log(N_{GPU})$$

$$\Delta T_{GPU} \propto N \cdot \frac{N_{act}}{N_{GPU}}$$

ftp://ftp.mao.kiev.ua/pub/berczik/phi-GPU/

Our φGRAPE/GPU N-body code

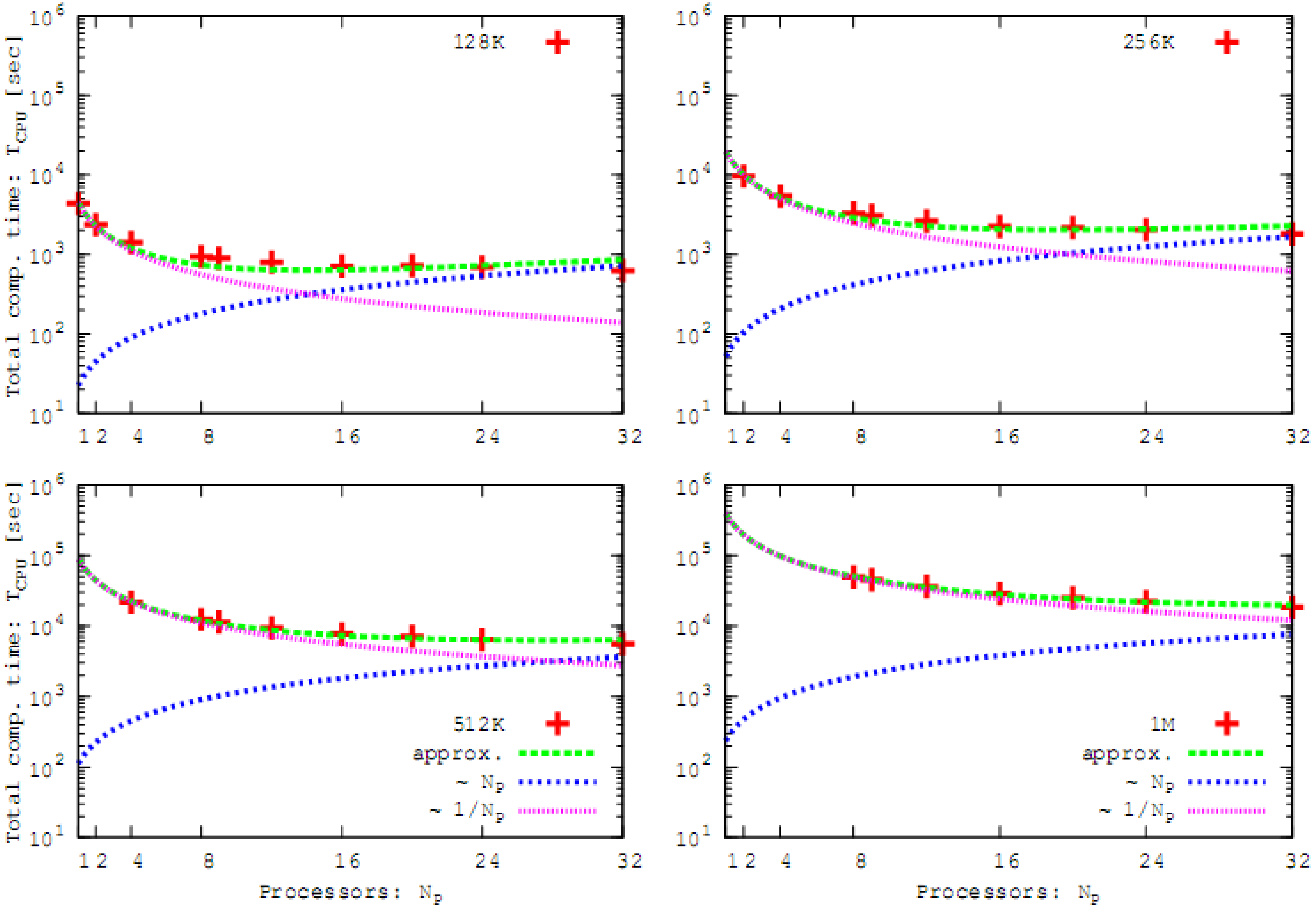

Our φGRAPE/GPU N-body code

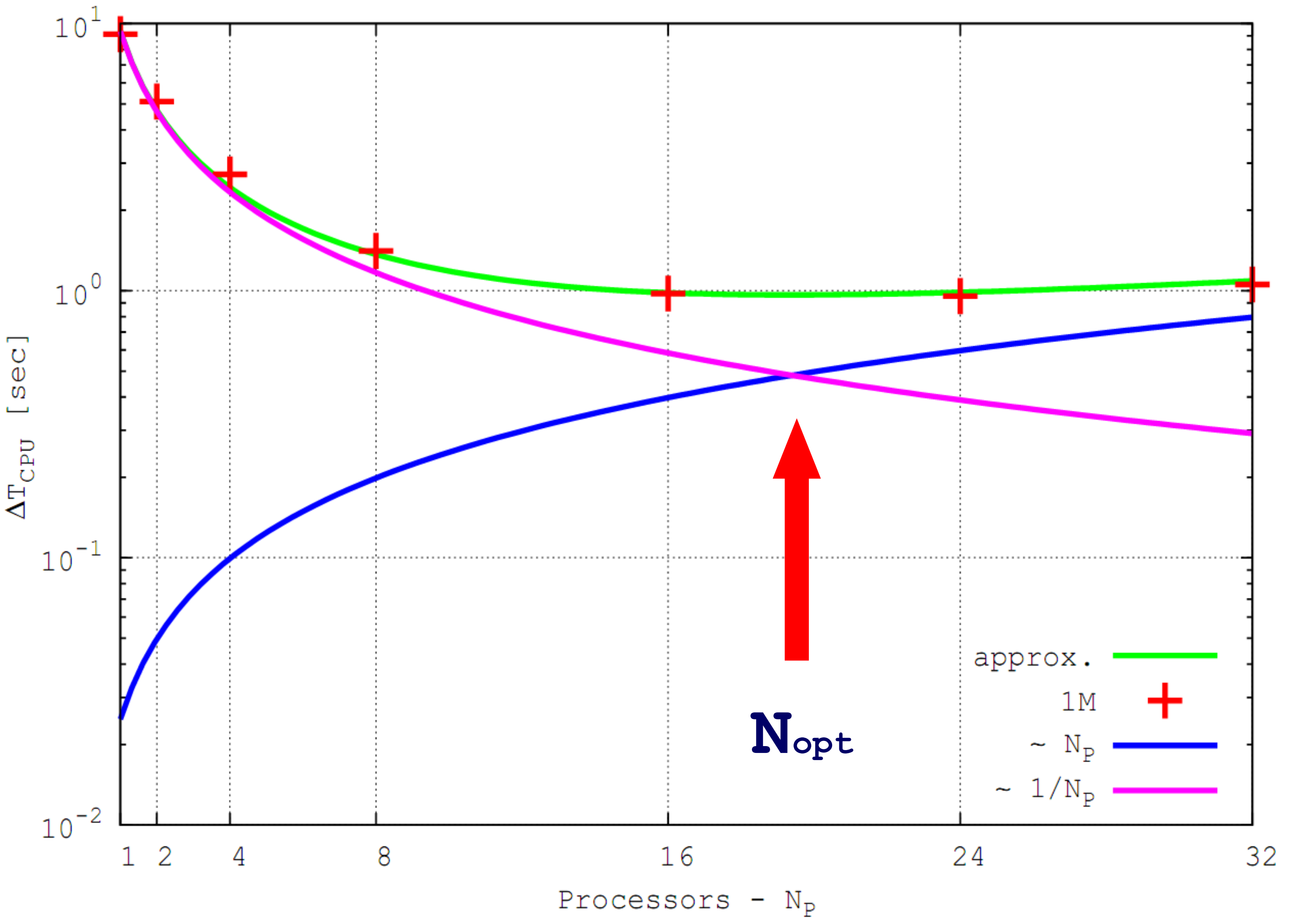

Our φGRAPE/GPU N-body code

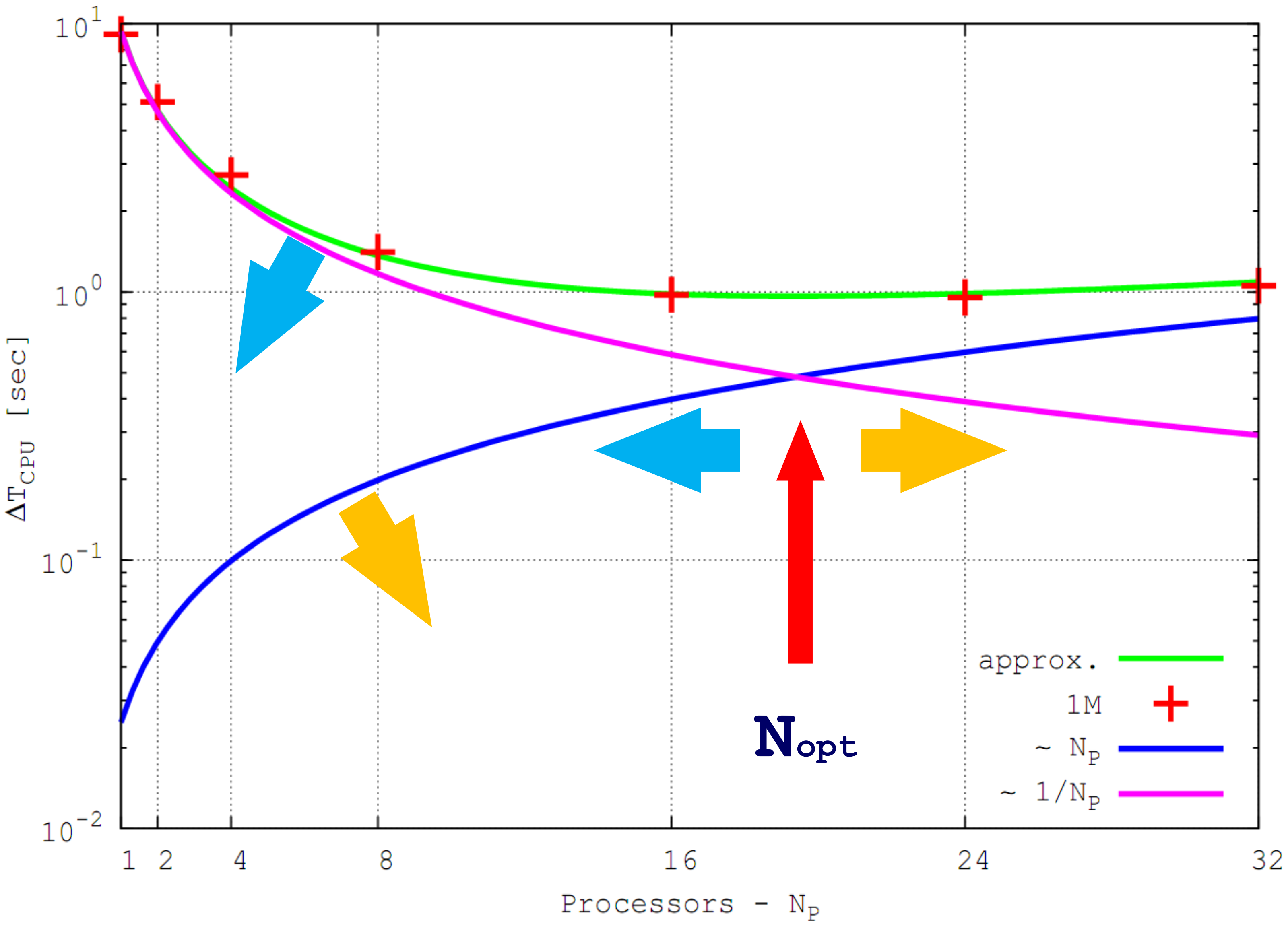

Initial Condition

$$M(r) = M_o \cdot \frac{1}{(1+(r_o/r)^2)^{3/2}}$$

$$\rho(r) = \frac{3 \cdot M_o}{4\pi \cdot r_o{}^3} \cdot \frac{1}{(1+(r/r_o)^2)^{5/2}}$$

$$r_{HM} \approx 0.769$$

$$G = M = 1$$

$$E_{TOT} = -\frac{1}{4}$$

$$r_o = \frac{3\pi}{16} \approx 0.6$$

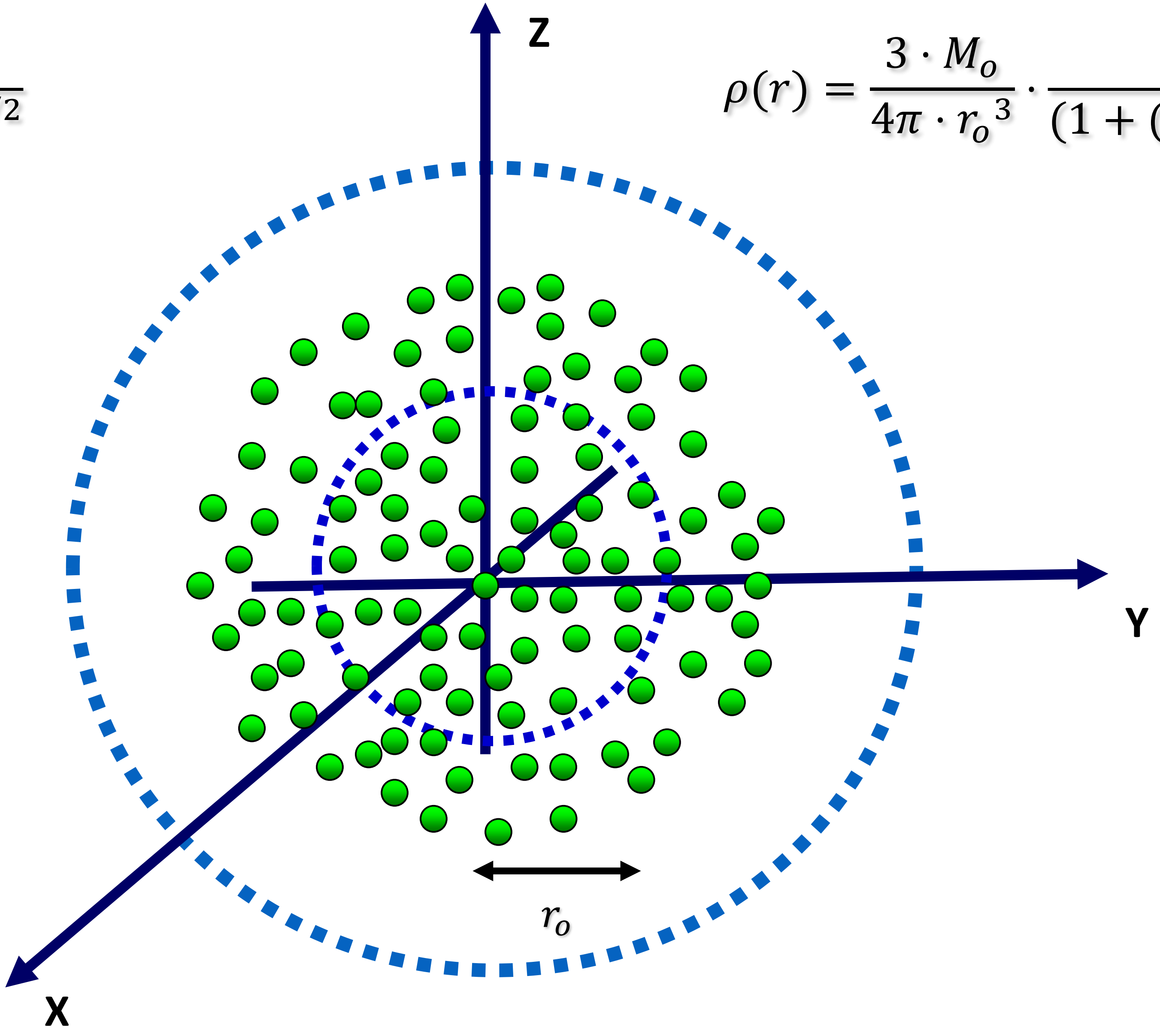

Initial Condition

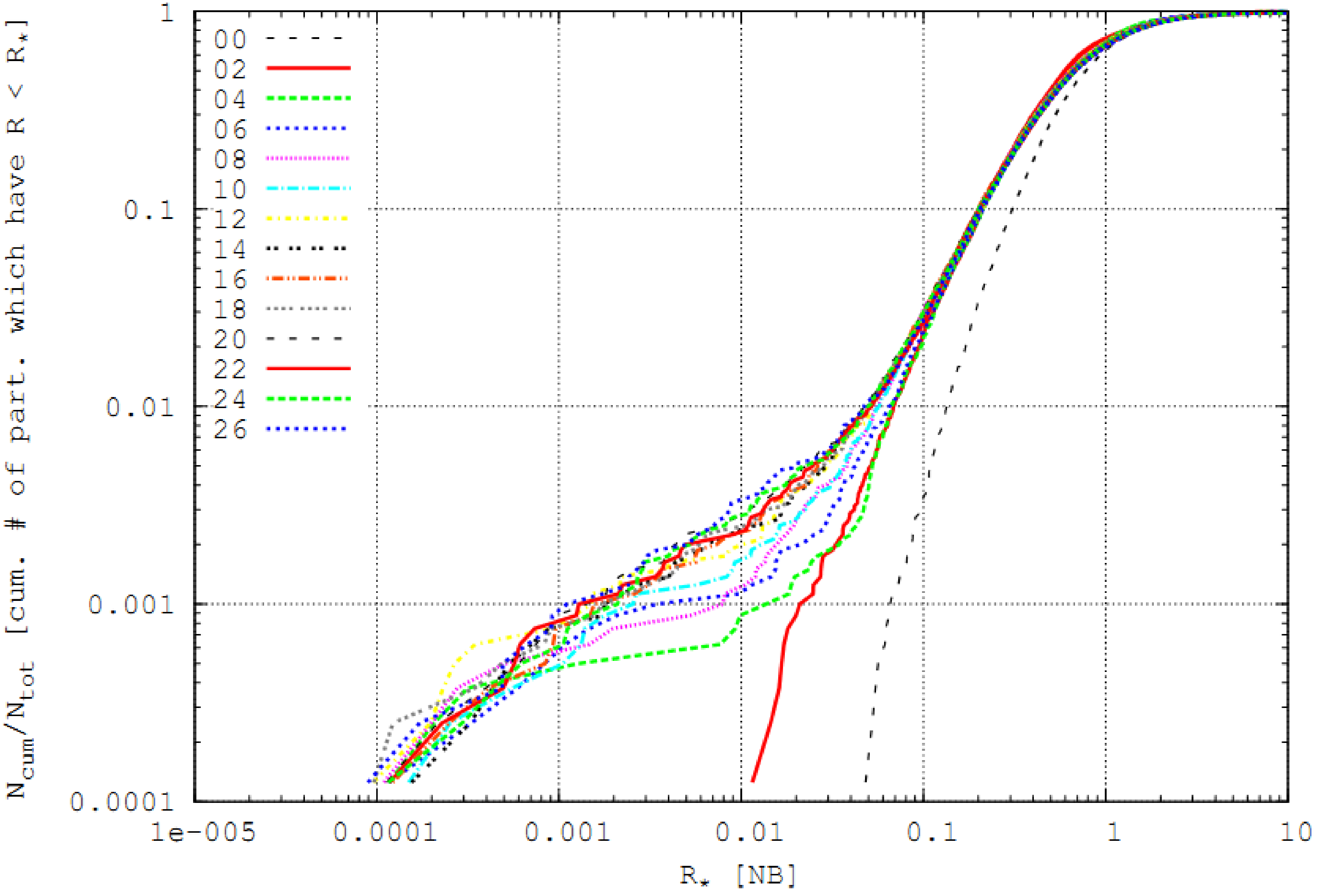

Initial Condition

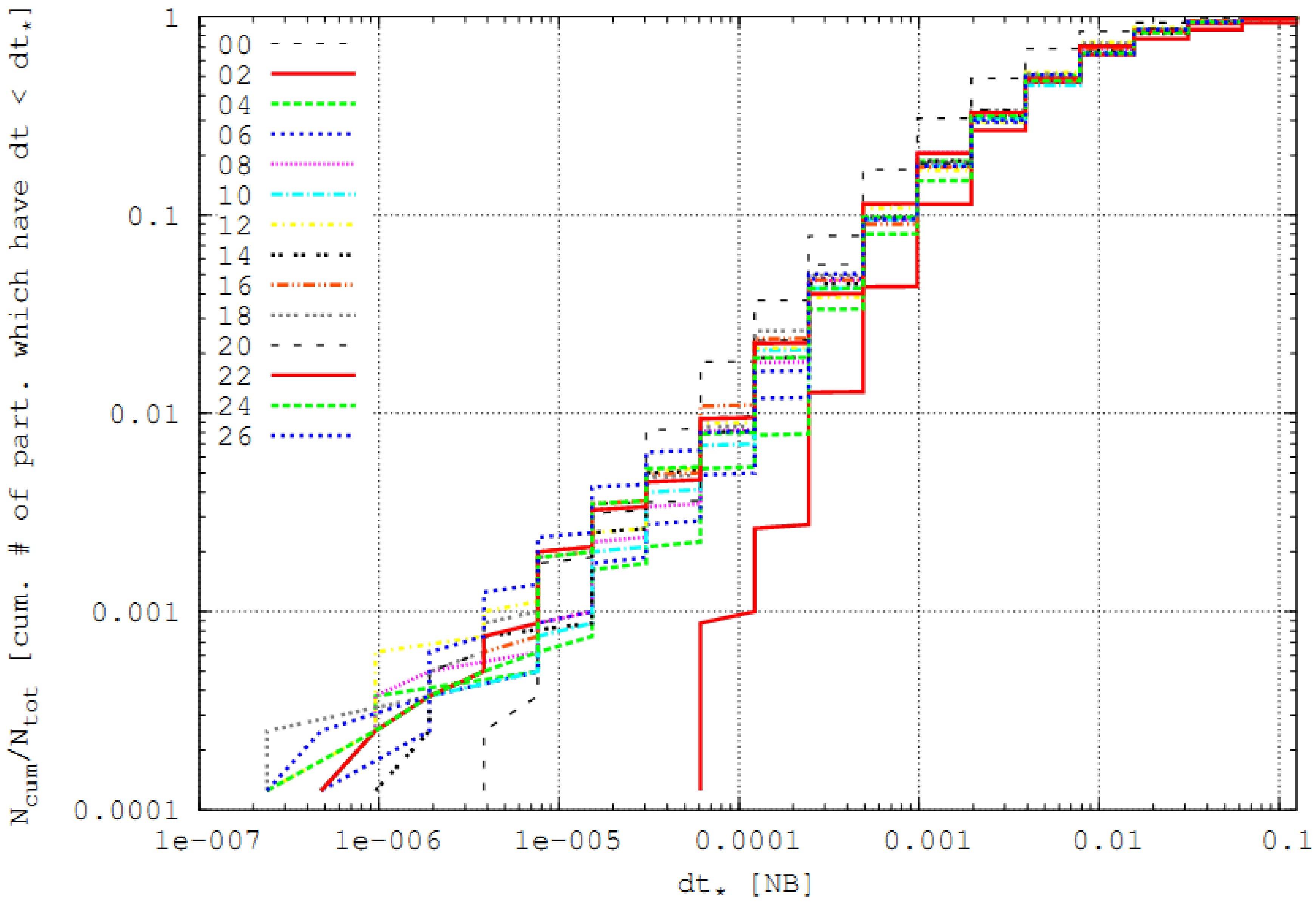

Our CPU/GPU "hybrid" N-body code

$$M(r) = M_o \cdot \frac{1}{(1+(r_o/r)^2)^{3/2}}$$

$$\rho(r) = \frac{3 \cdot M_o}{4\pi \cdot r_o{}^3} \cdot \frac{1}{(1+(r/r_o)^2)^{5/2}}$$

$$r_{HM} \approx 0.769$$

$$G = M = 1$$

$$E_{TOT} = -\frac{1}{4}$$

$$r_o = \frac{3\pi}{16} \approx 0.6$$

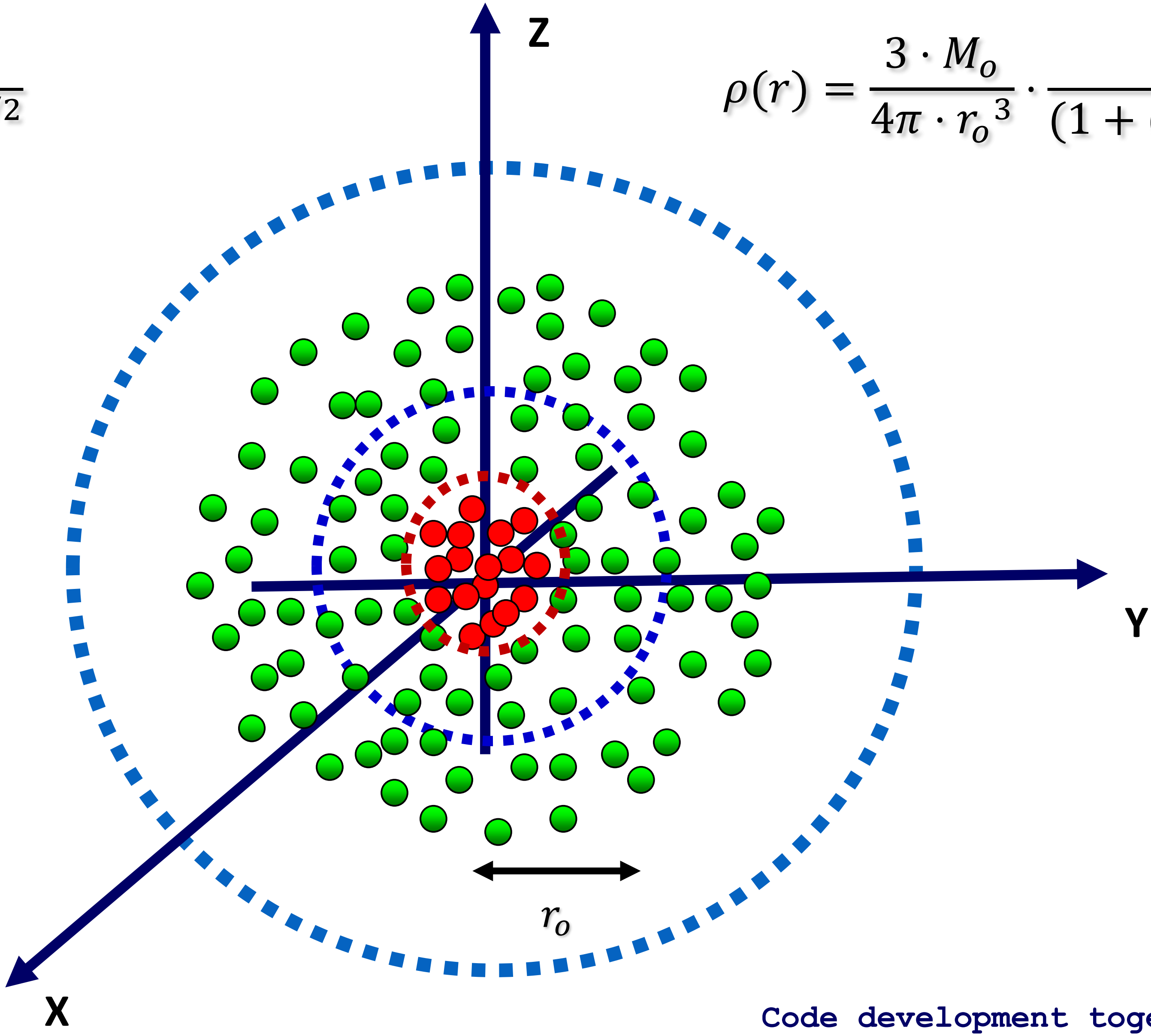

Code development together with Yohai…

Our CPU/GPU "hybrid" N-body code

$$M(r) = M_o \cdot \frac{1}{(1+(r_o/r)^2)^{3/2}}$$

$$\rho(r) = \frac{3 \cdot M_o}{4\pi \cdot {r_o}^3} \cdot \frac{1}{(1+(r/r_o)^2)^{5/2}}$$

$$r_{HM} \approx 0.769$$

$$G = M = 1$$

$$E_{TOT} = -\frac{1}{4}$$

$$r_o = \frac{3\pi}{16} \approx 0.6$$

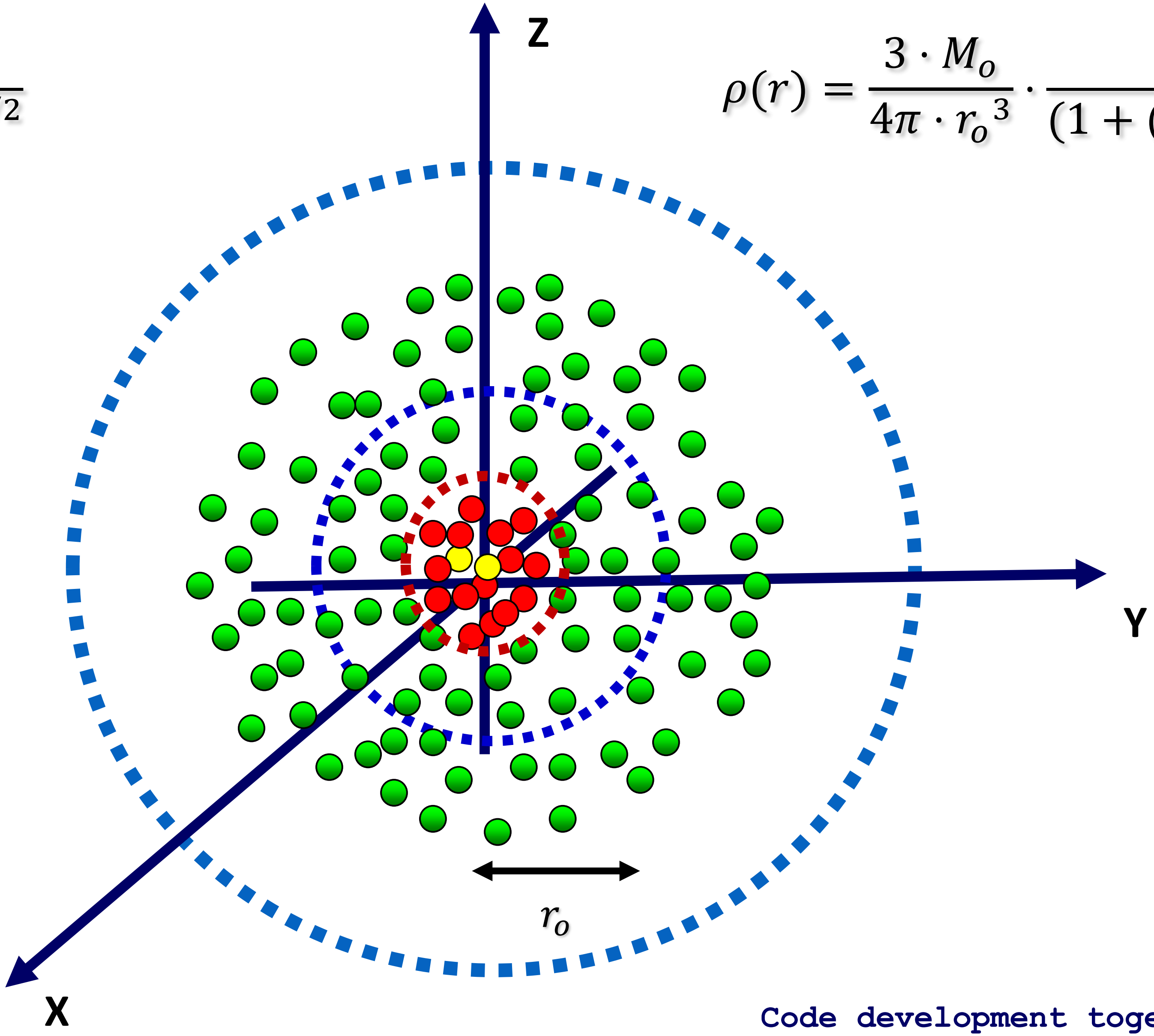

Code development together with Yohai…

Our CPU/GPU "hybrid" N-body code

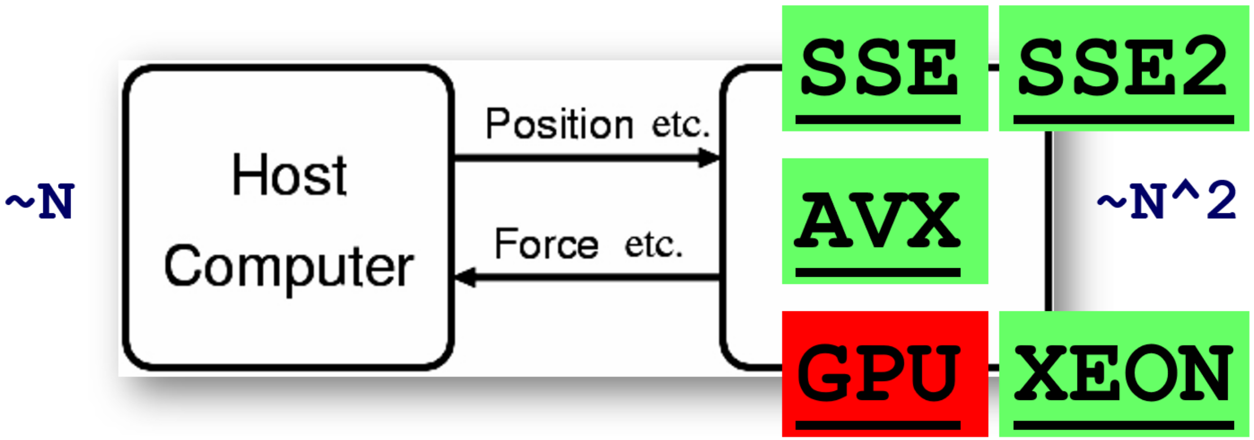

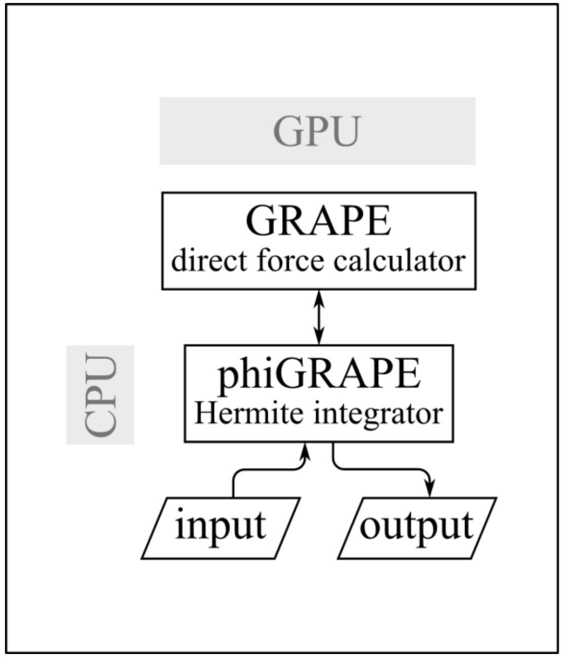

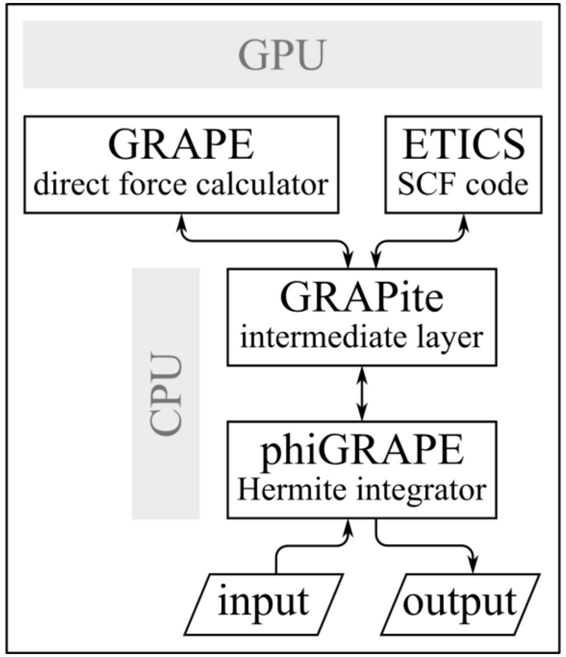

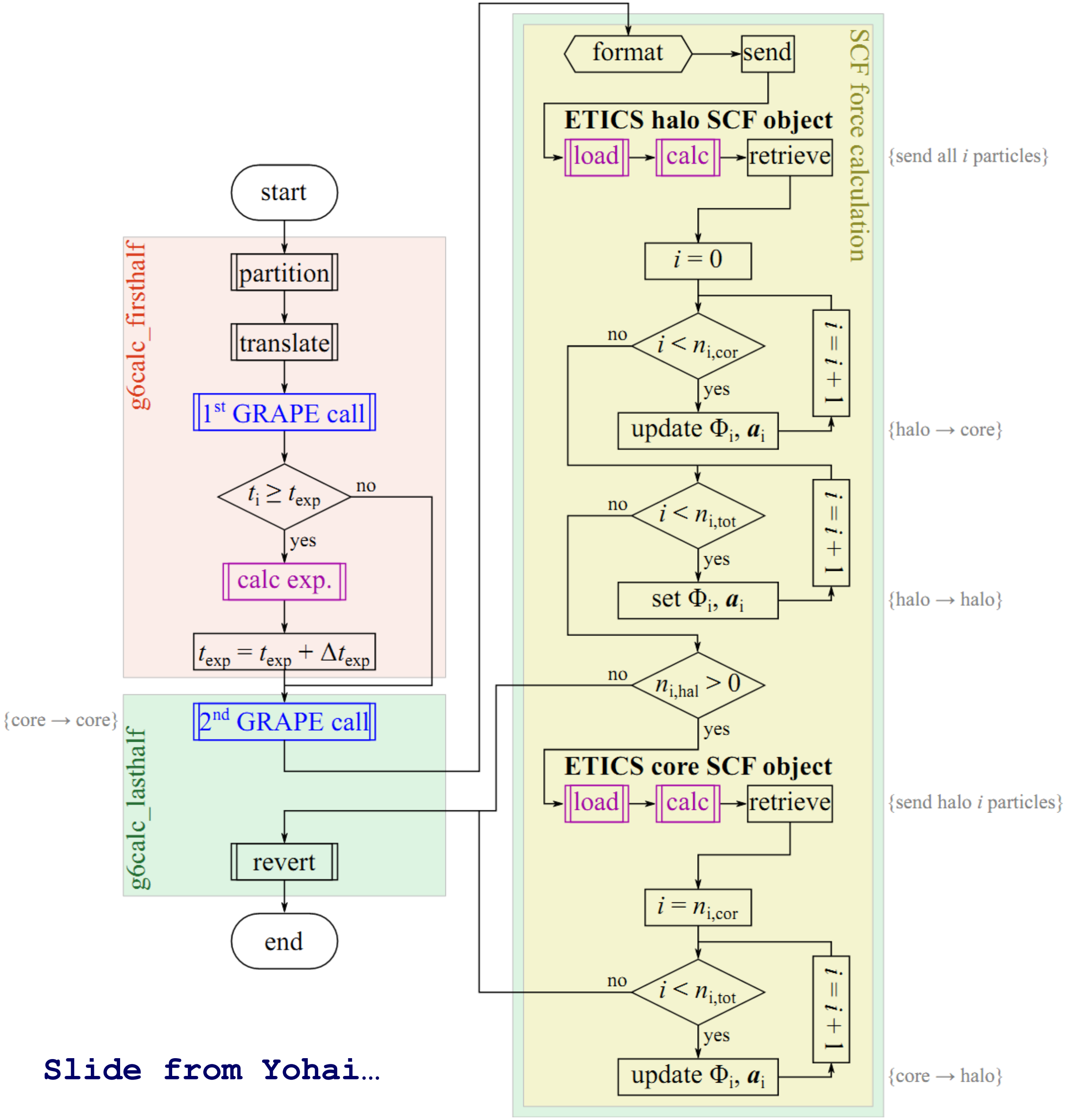

Slide from Yohai…

Double & Triple SMBH evolution in galaxy centers. New hybrid code approaches and performance tests.

MAO 3+2 new nodes 4xGF 2080S + 4xGF 3070

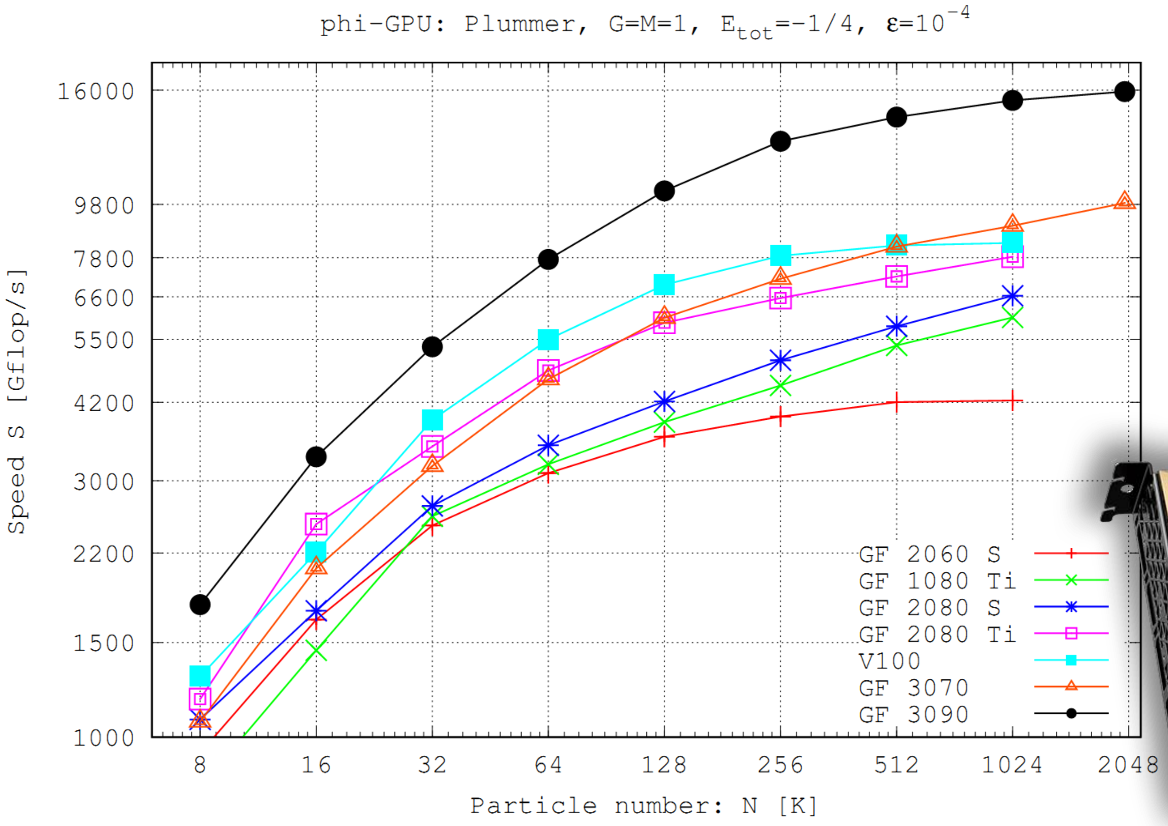

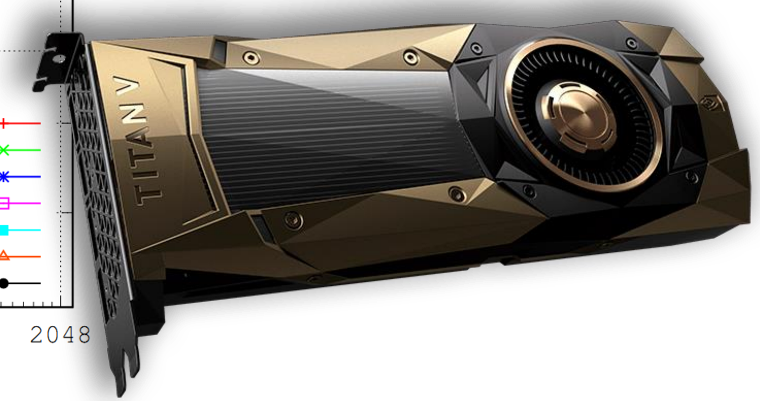

4 x GF 2080S, 3072 SP @ 1.81 GHz
4 x GF 3070, 5888 SP @ 1.77 GHz

JUWELS Booster consists of 936 compute nodes, each equipped with 4 NVIDIA A100 GPUs. The GPUs are hosted by AMD EPYC Rome CPUs. The compute nodes are connected with HDR-200 InfiniBand in a DragonFly+ topology.

The InfiniBand network of JUWELS Booster is implemented as a DragonFly+ network.

48 nodes are combined in a switch group (*cell*), interconnected in a full fat-tree topology, with 10 leaf switches and 10 spine switches in a two-level configuration. 40 Tbit/s of bi-section bandwidth is available.

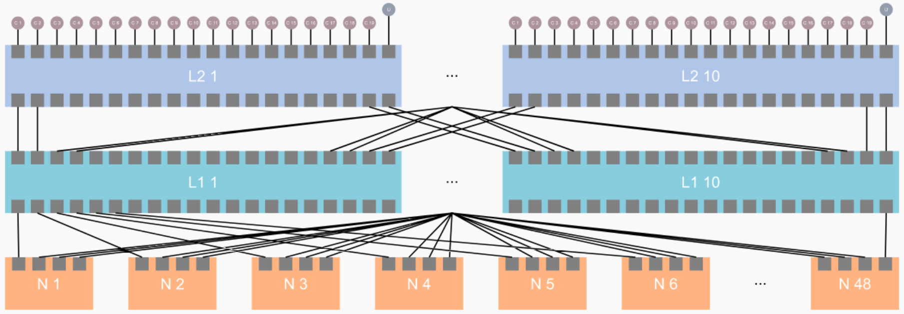

Sketch of the network topology within a JUWELS Booster cell with 48 nodes (`N1` to `N 48`), 10 level 1 switches (`L1 1` to `L1 10`) and 10 level 2 switches (`L2 1` to `L2 10`). Only a small subset of the total amount of links are shown for readability. The purple, 20th link leaving each level 2 switch should indicate the connection to JUWELS Cluster, while the other 19 outgoing level 2 links connect to other cells.

The configuration of JUWELS Booster compute nodes is the following

- **CPU**: AMD EPYC 7402 processor; 2 sockets, 24 cores per socket, SMT-2 (total: 2×24×2 = 96 threads) in NPS-4 [1] configuration (details on WikiChip)
- **Memory**: 512 GB DDR4-3200 RAM (of which at least 20 GB is taken by the system software stack, including the file system); 256 GB per socket; 8 memory channels per socket (2 channels per NUMA domain)
- **GPU**: 4 × NVIDIA A100 Tensor Core GPU with 40 GB; connected via NVLink3 to each other
- **Network**: 4 × Mellanox HDR200 InfiniBand ConnectX 6 (200 Gbit/s each), *HCA*
- **Periphery**: CPU, GPU, and network adapter are connected via 2 PCIe Gen 4 switches with 16 PCIe lanes going to each device (CPU socket: 2×16 lanes). PCIe switches are configured in *synthetic mode*.

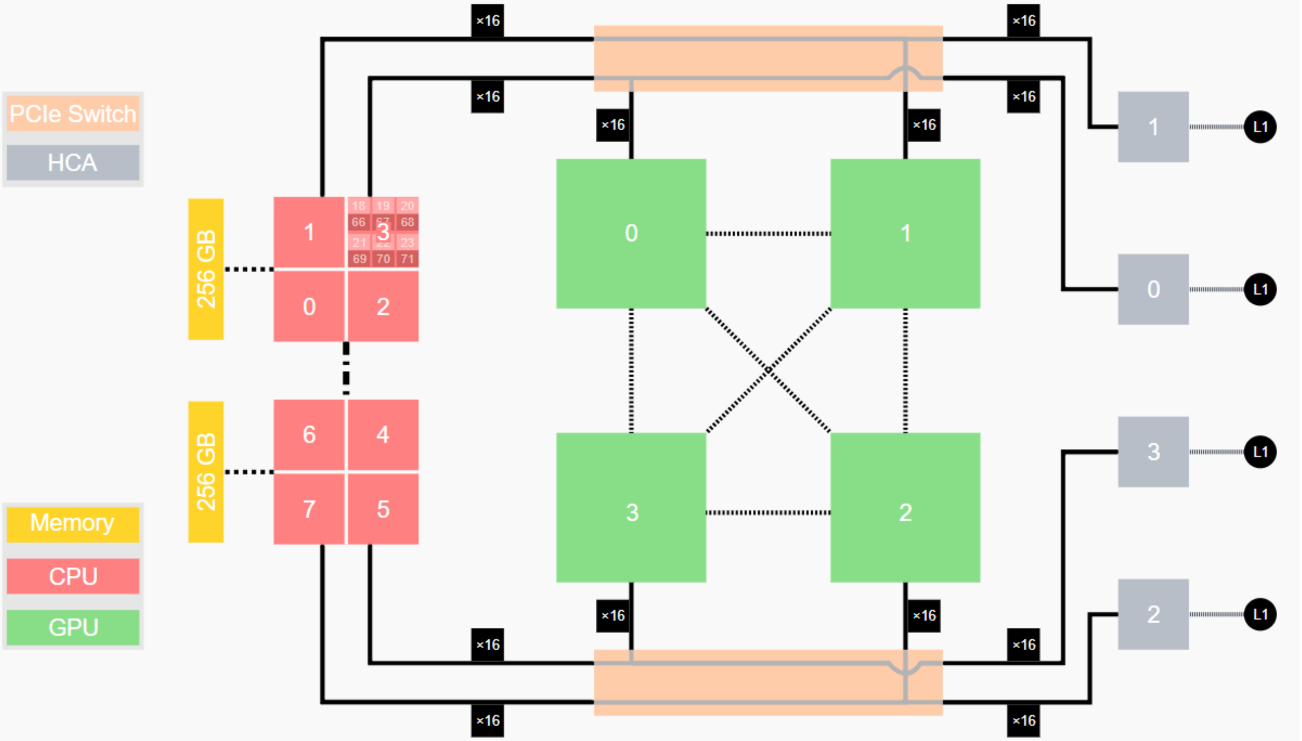

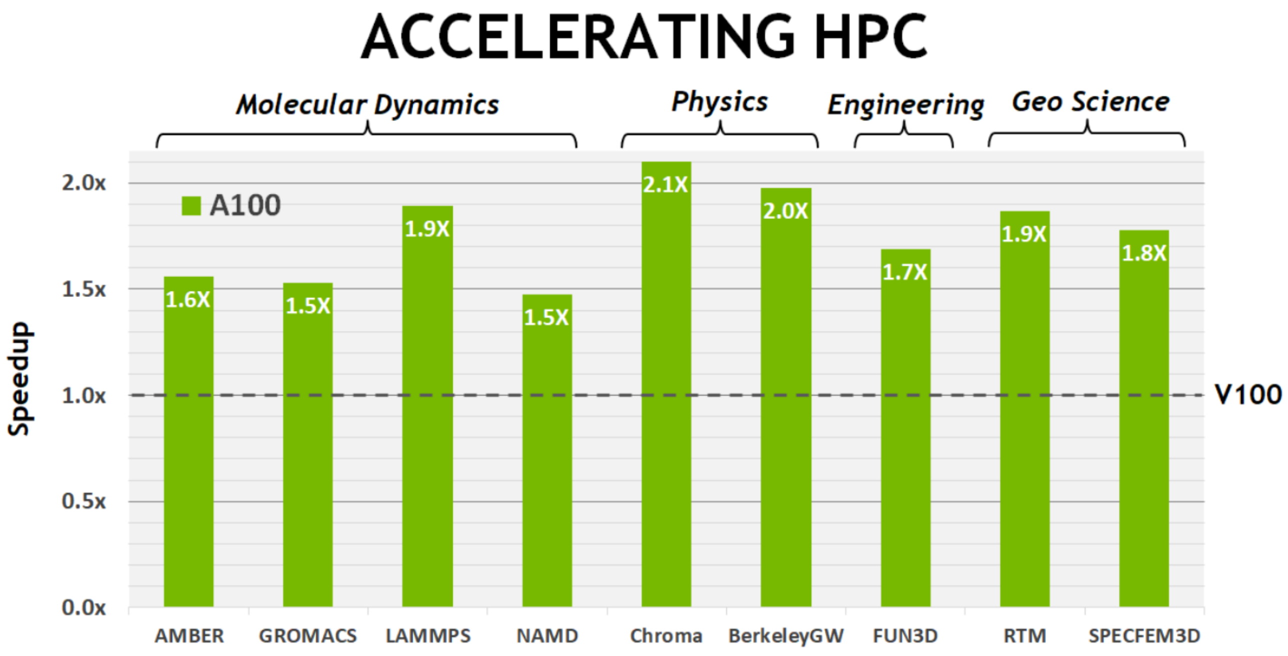

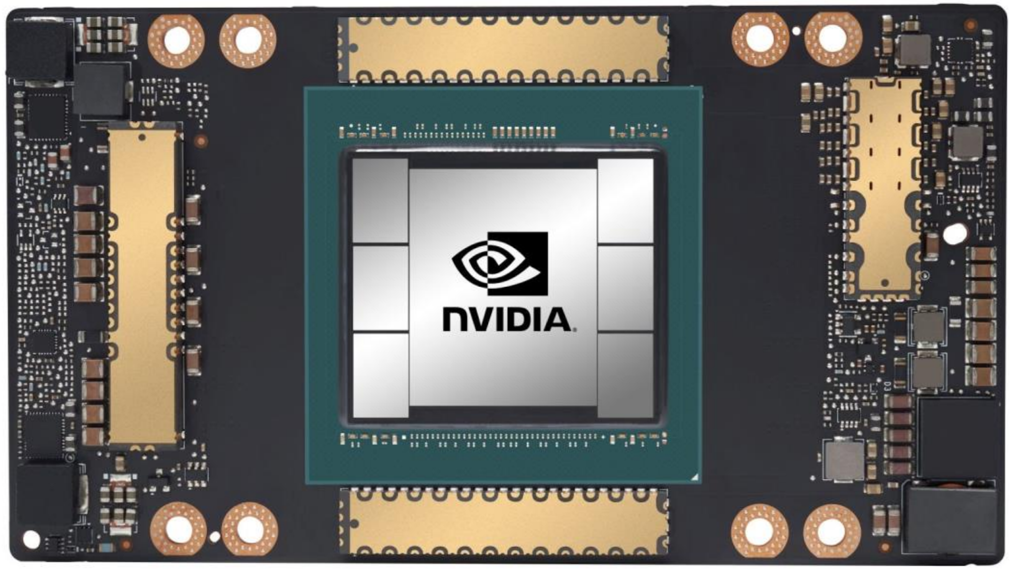

Peak FP64[1]	9.7 TFLOPS
Peak FP64 Tensor Core[1]	19.5 TFLOPS
Peak FP32[1]	19.5 TFLOPS
Peak FP16[1]	78 TFLOPS
Peak BF16[1]	39 TFLOPS
Peak TF32 Tensor Core[1]	156 TFLOPS | 312 TFLOPS[2]
Peak FP16 Tensor Core[1]	312 TFLOPS | 624 TFLOPS[2]
Peak BF16 Tensor Core[1]	312 TFLOPS | 624 TFLOPS[2]
Peak INT8 Tensor Core[1]	624 TOPS | 1,248 TOPS[2]
Peak INT4 Tensor Core[1]	1,248 TOPS | 2,496 TOPS[2]

Table 1. A100 Tensor Core GPU performance specs.
1) Peak rates are based on the GPU boost clock.
2) Effective TFLOPS / TOPS using the new Sparsity feature.

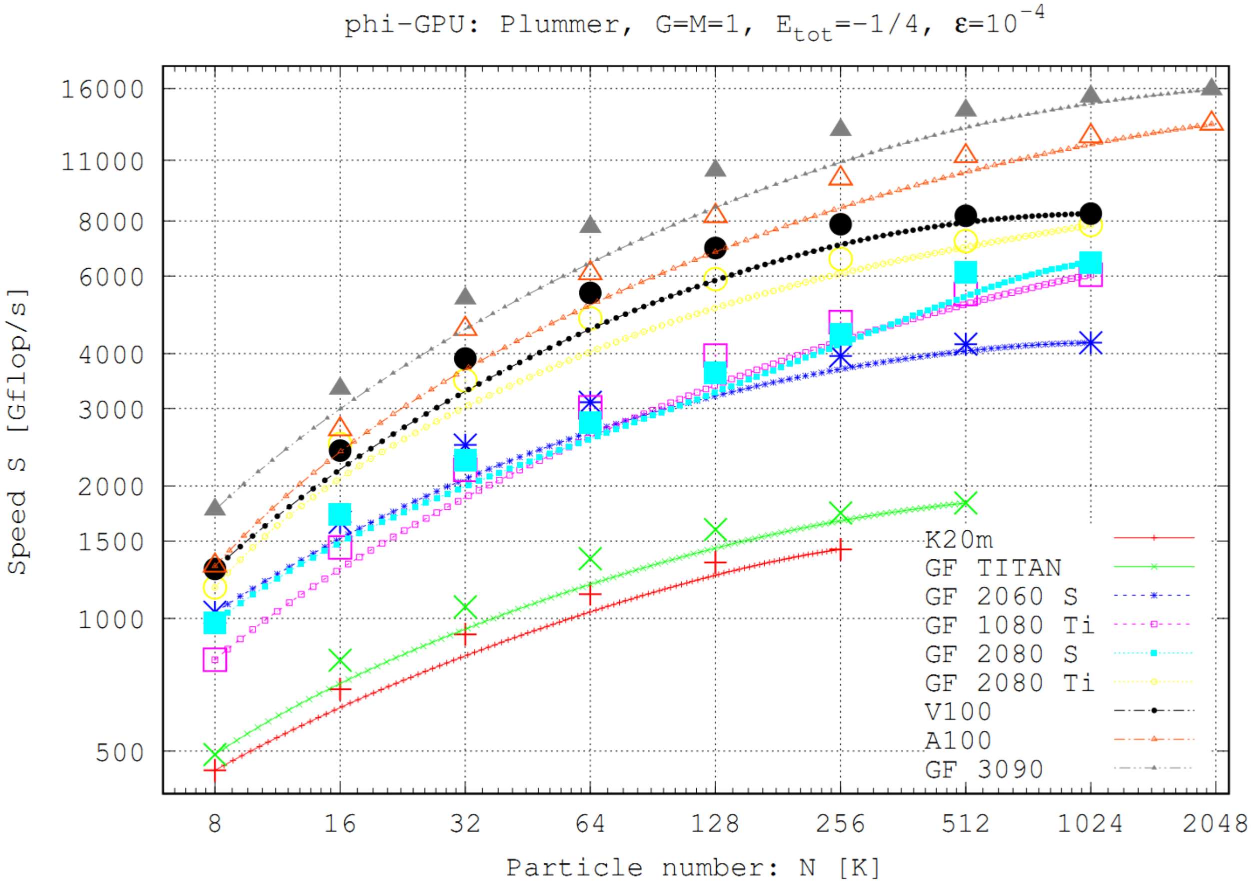

Our φGRAPE/GPU (single node) N-body code

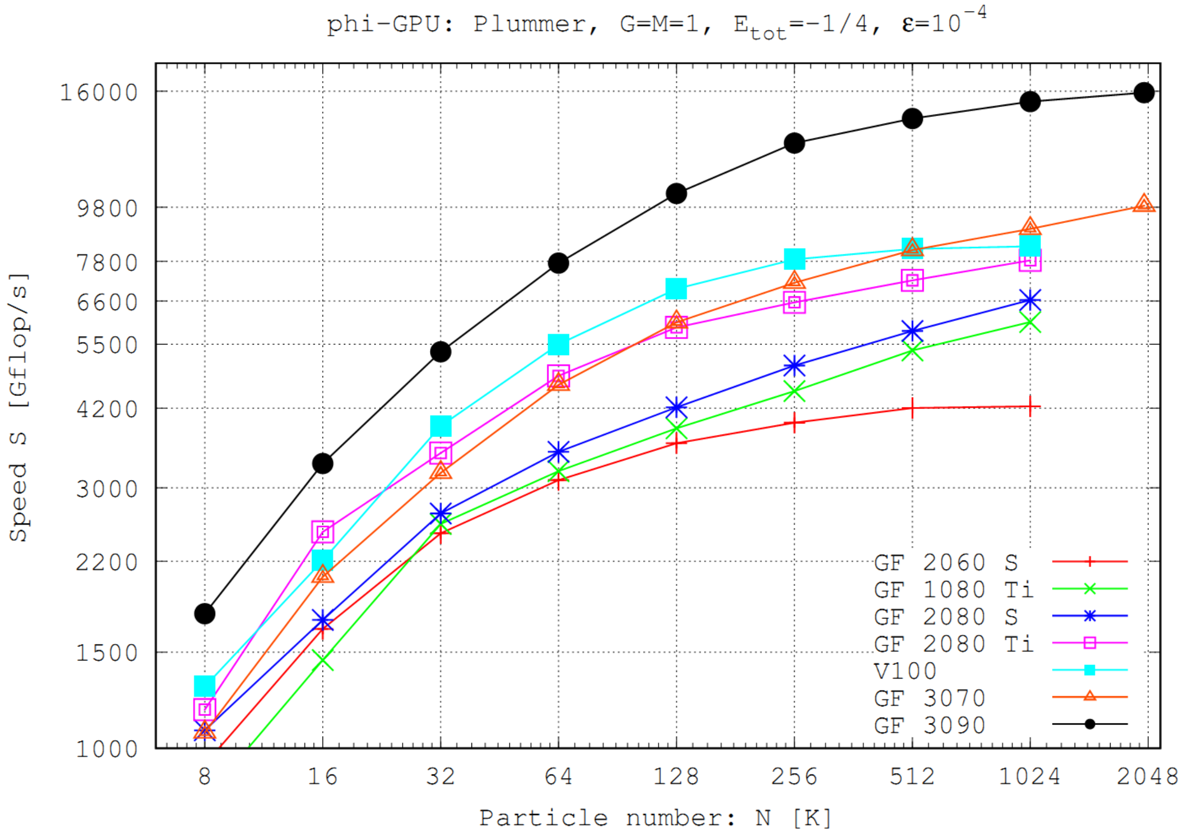

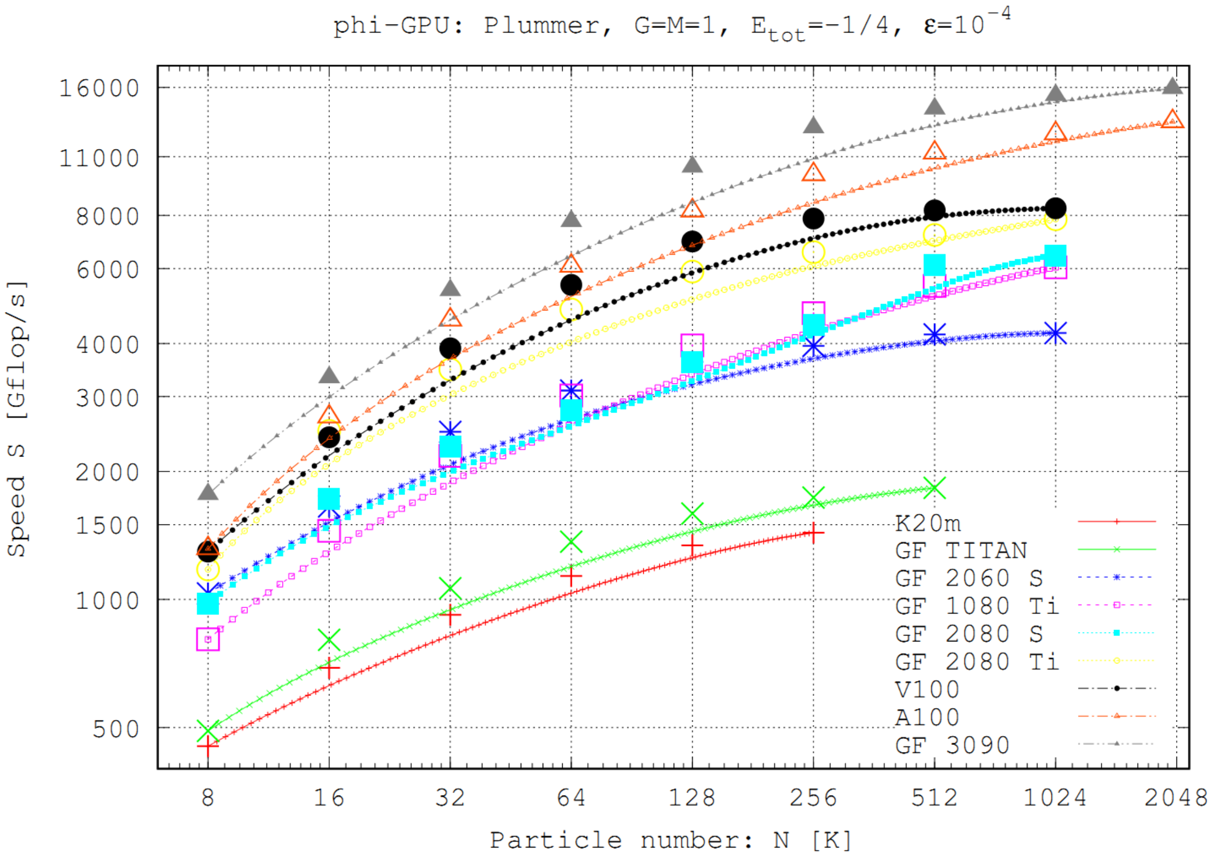

Our φGRAPE/GPU (single node) N-body code

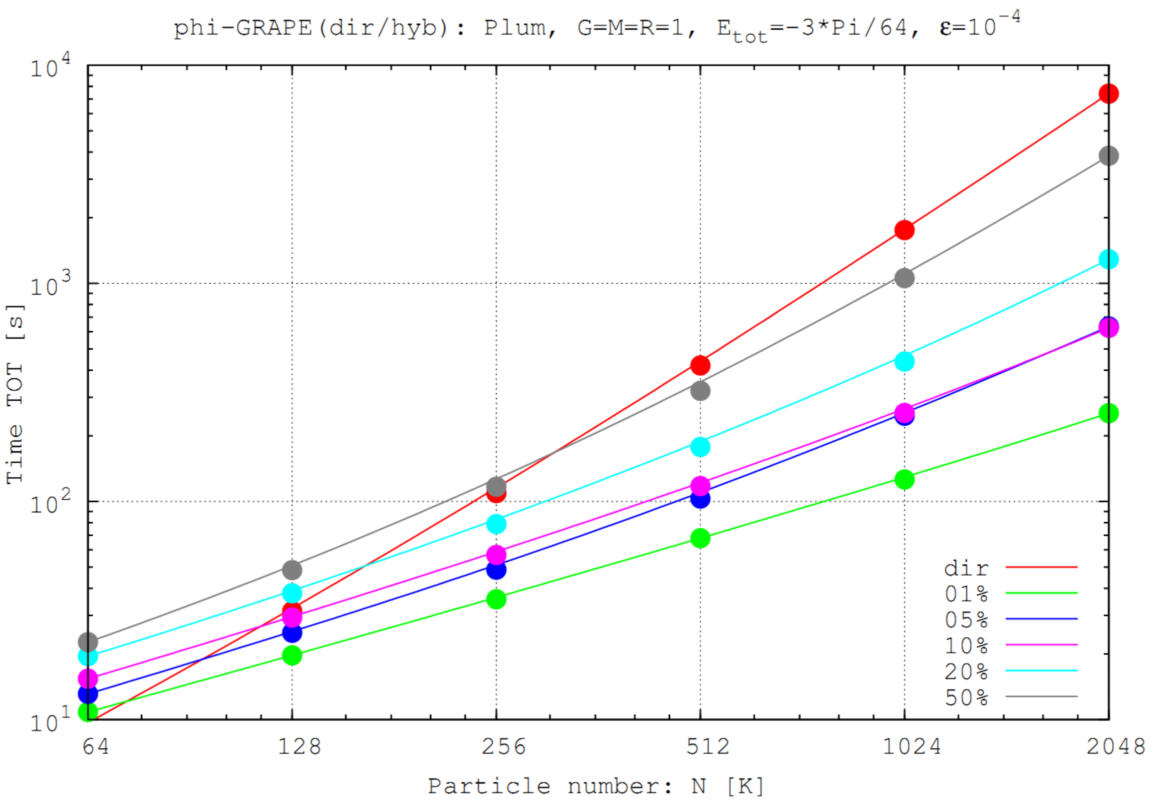

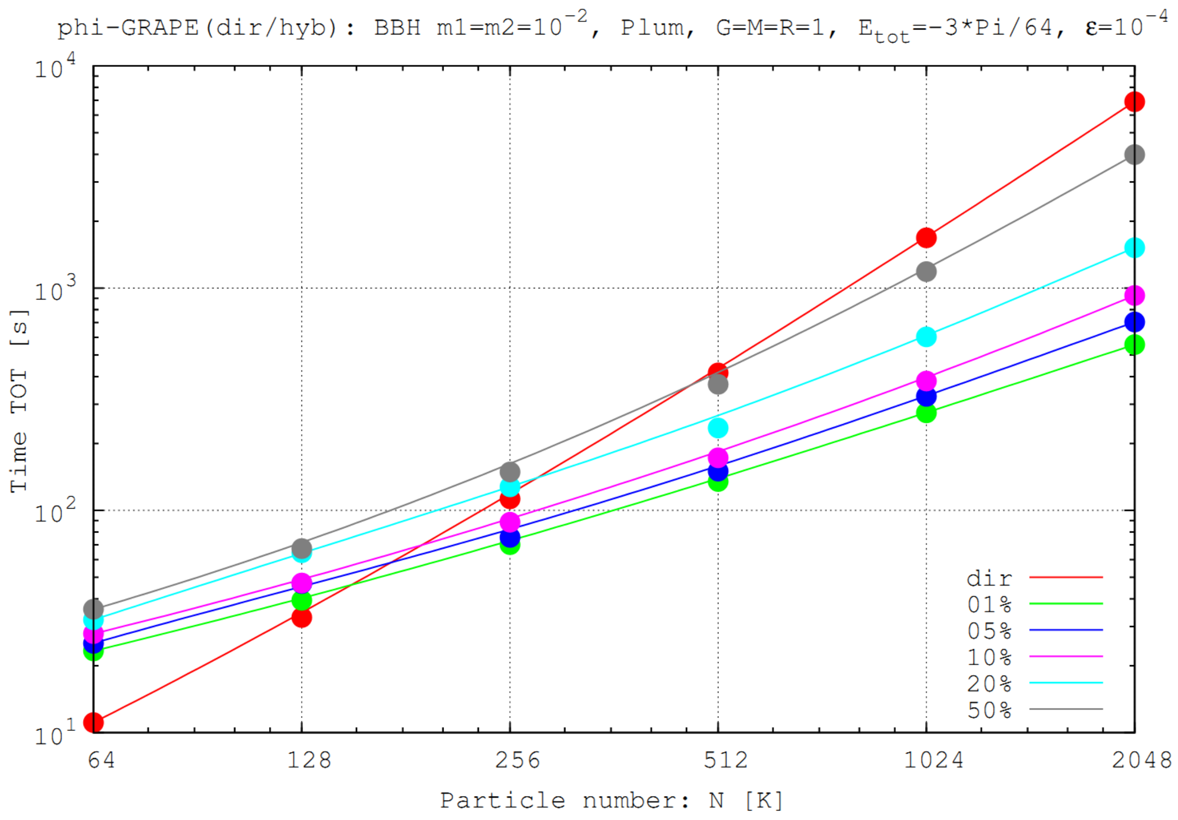

Our φGRAPE/GPU (single node) N-body code

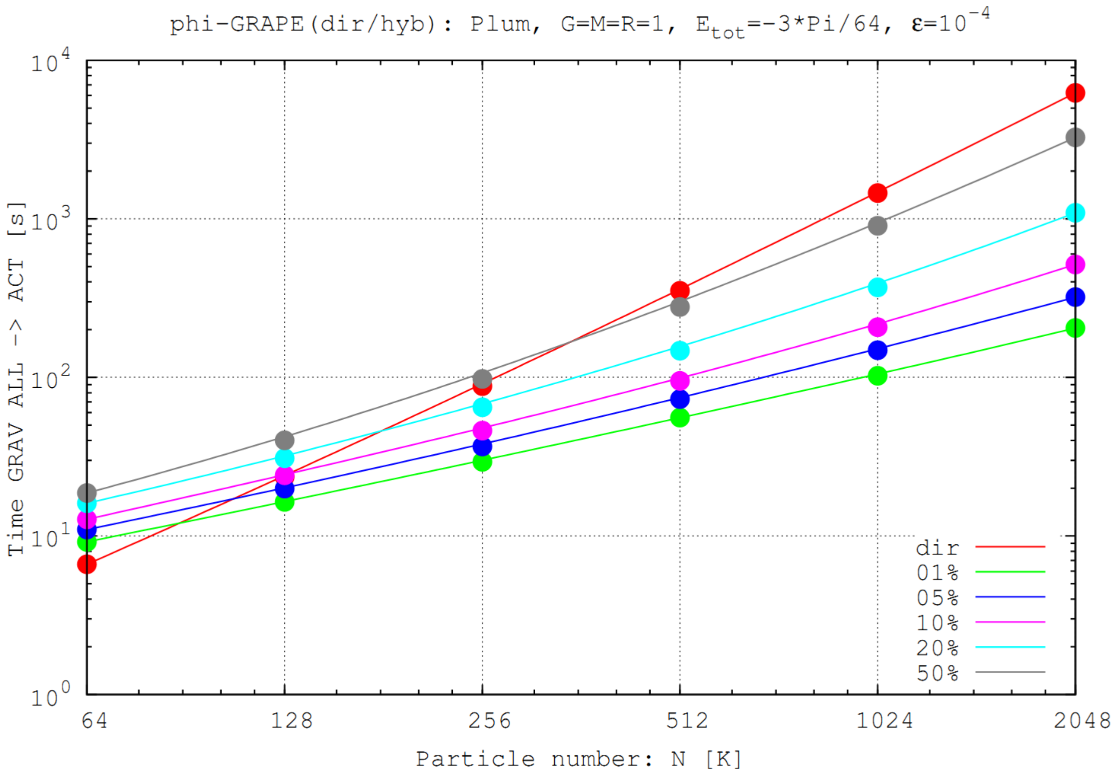

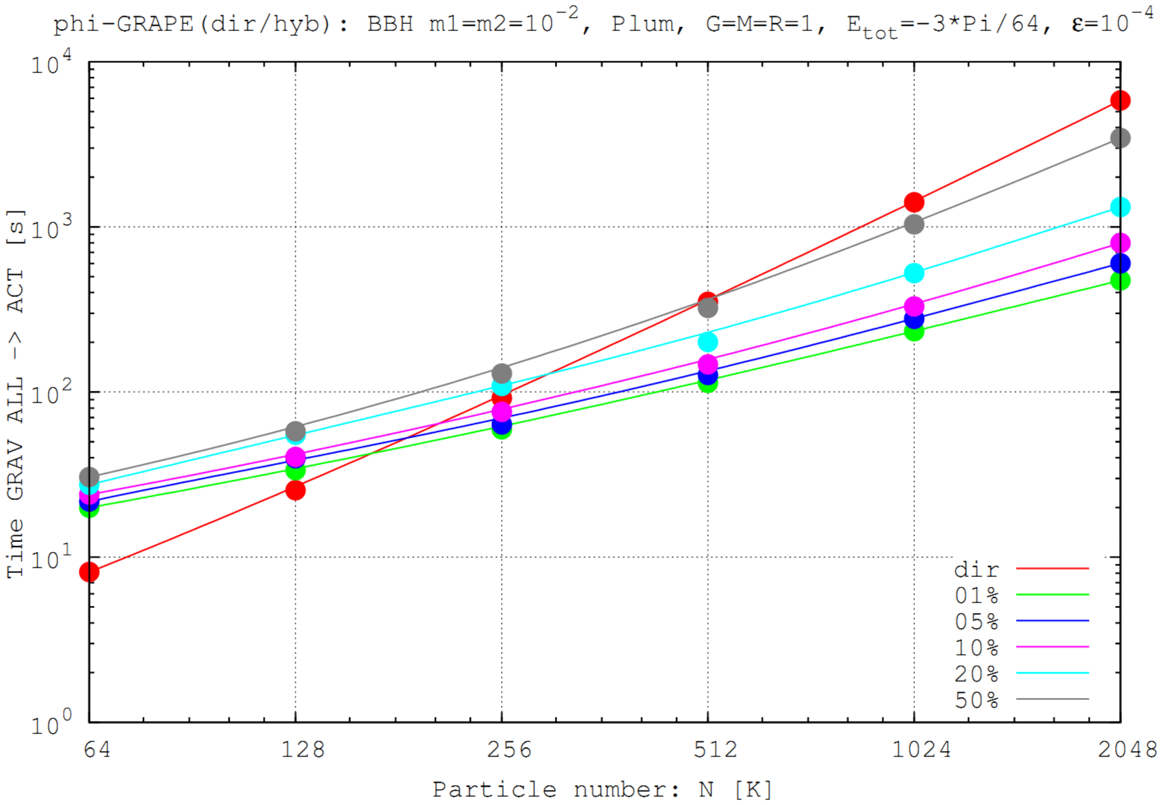

Our φGRAPE/GPU (single node) N-body code

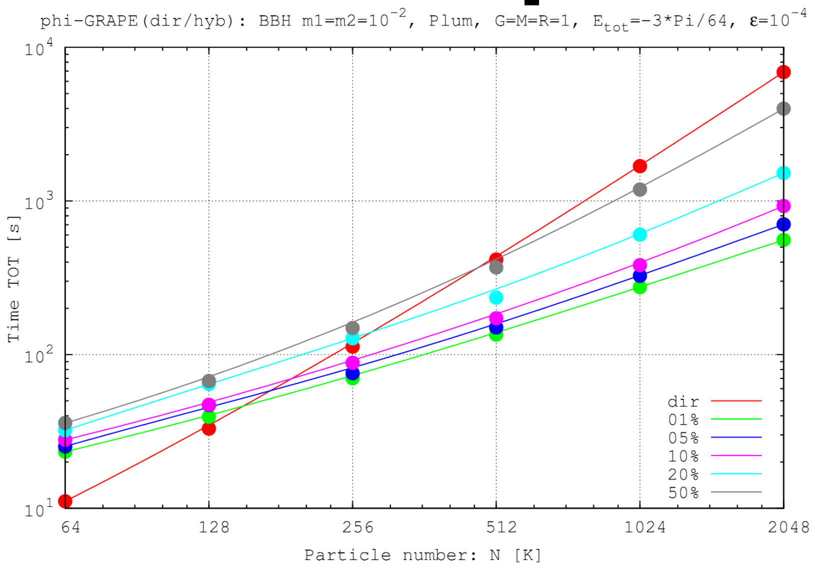

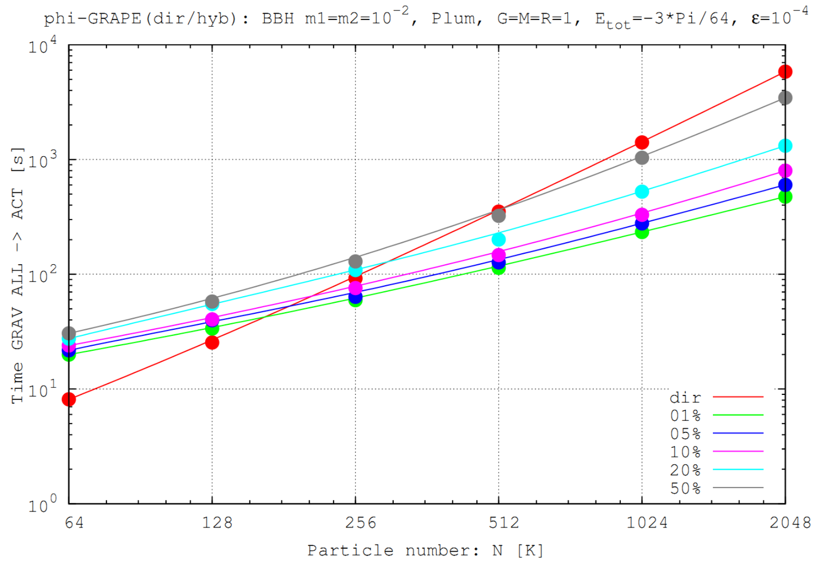

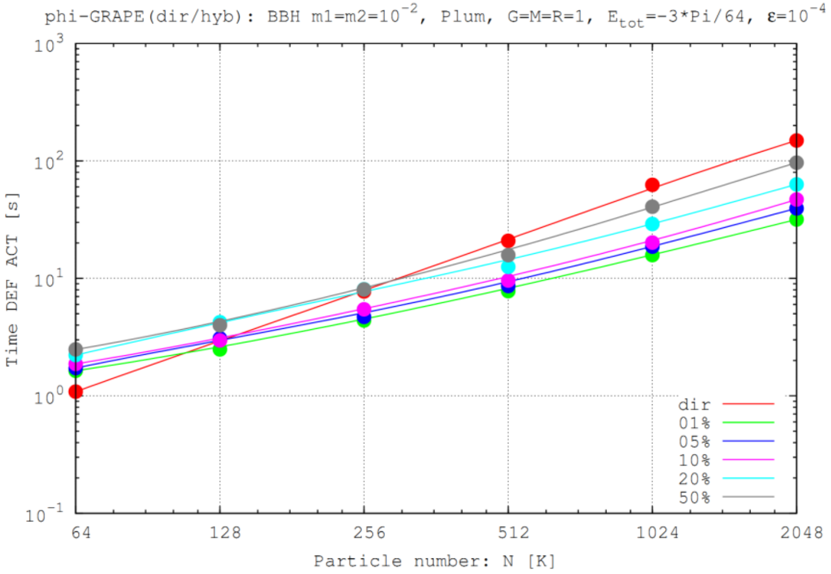

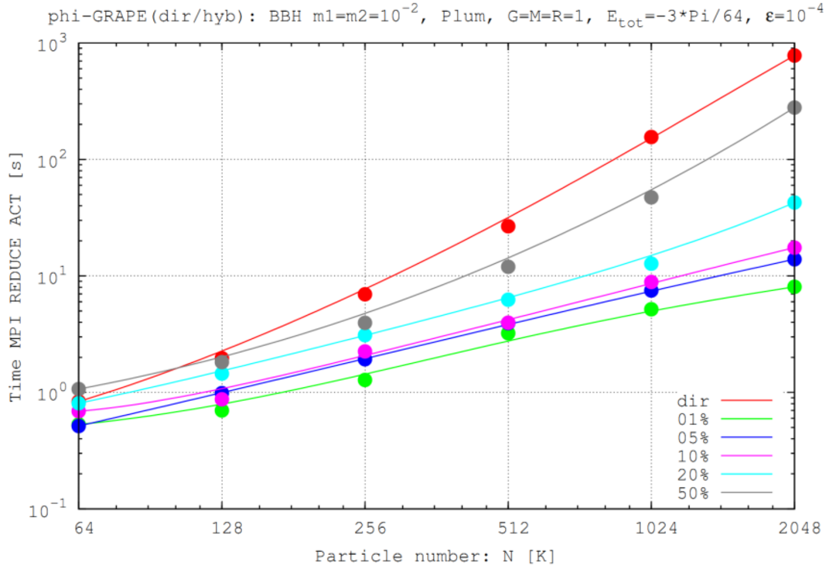

Our φGRAPE/GPU (parallel) N-body code

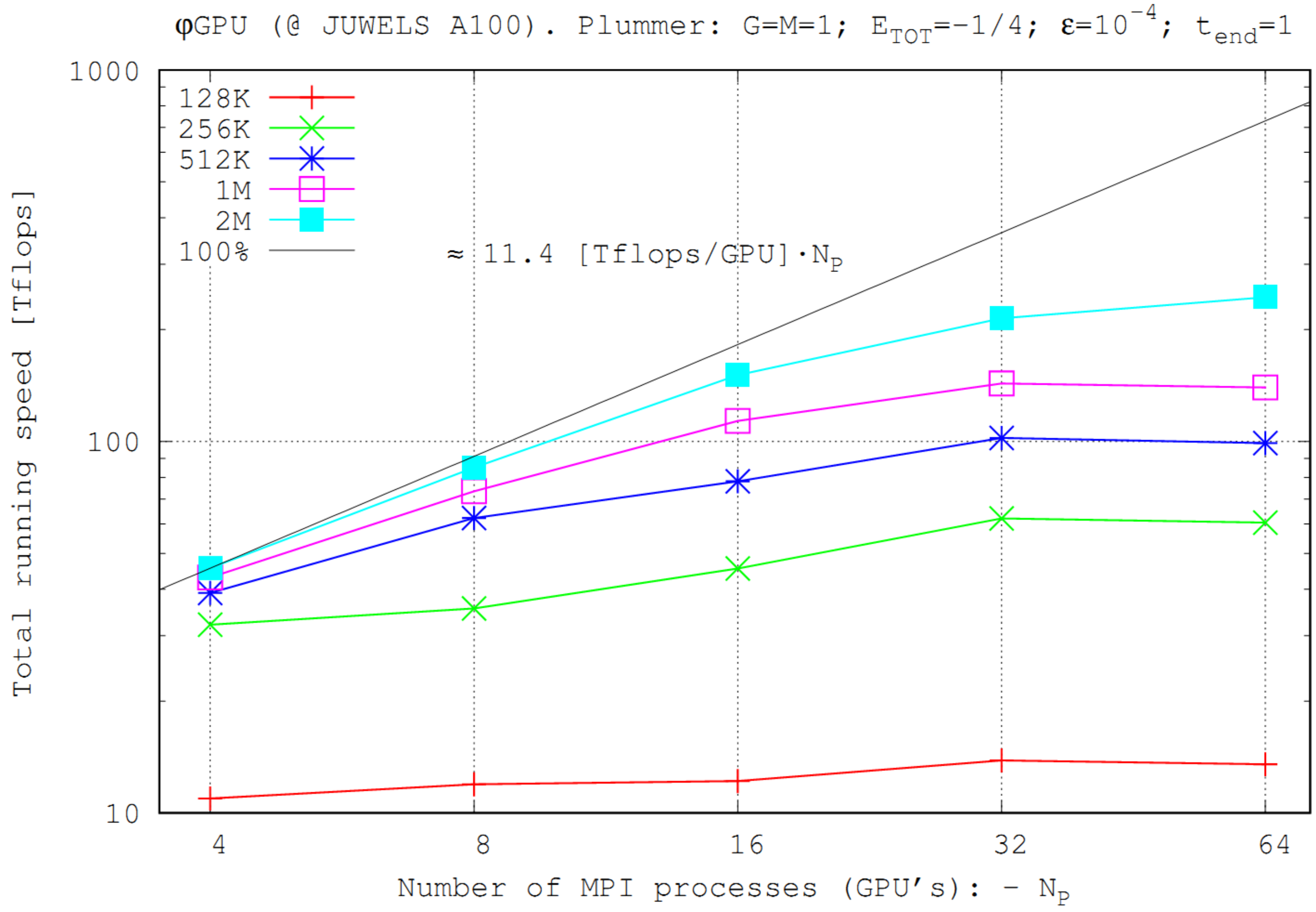

Our φGRAPE/GPU (parallel) N-body code

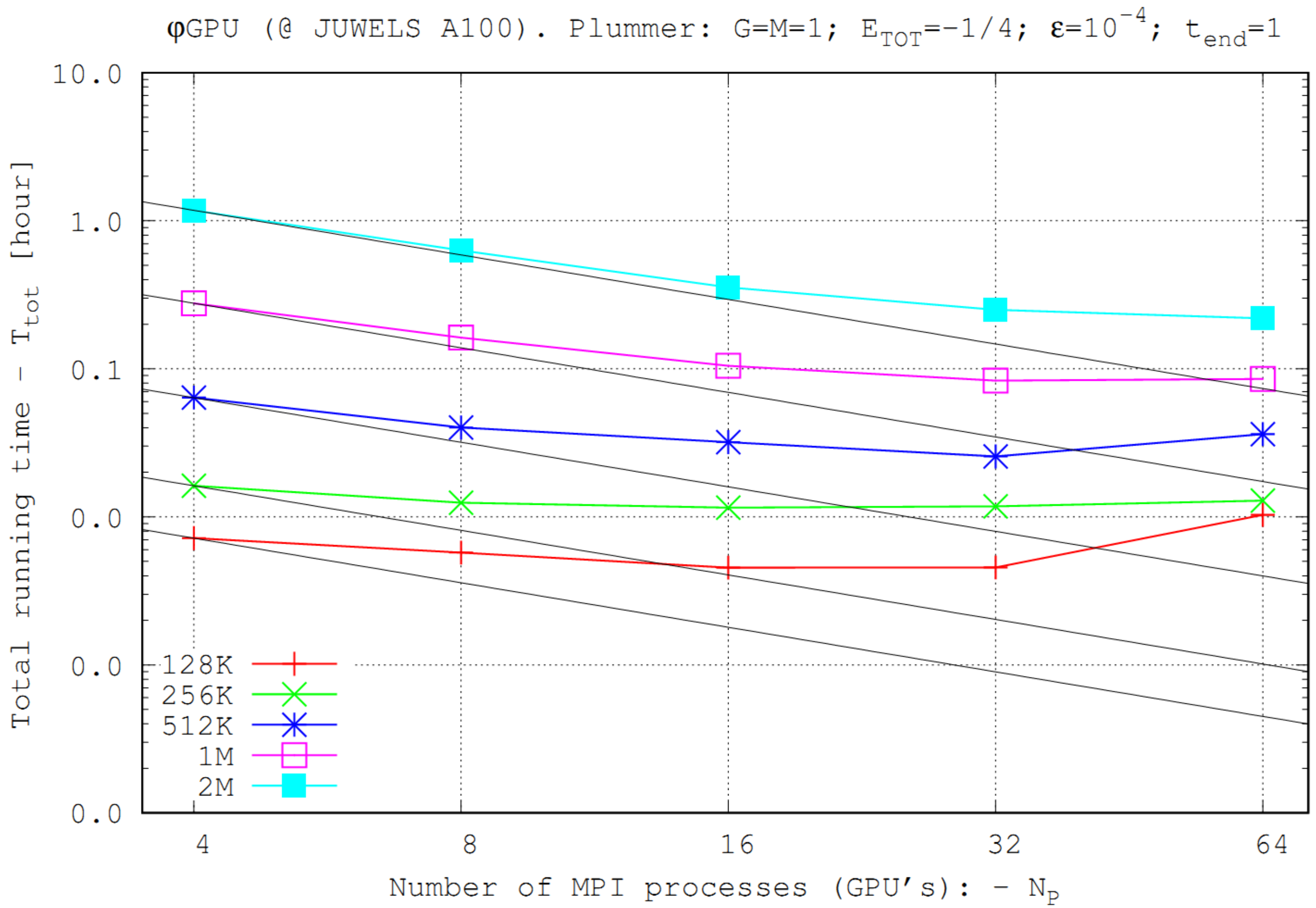

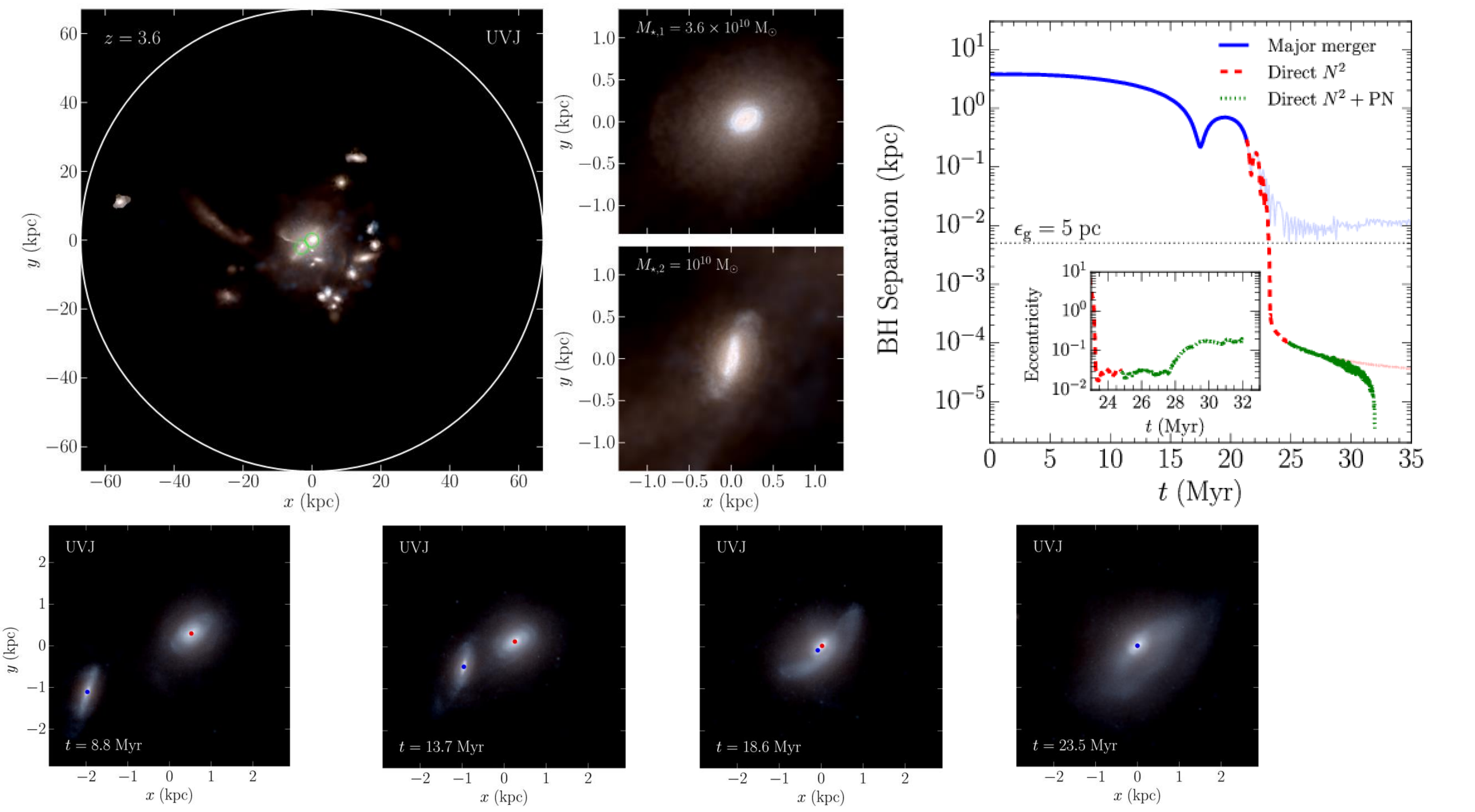

$z = 3.6$
UVJ
y (kpc)
x (kpc)
$M_{\star,1} = 3.6 \times 10^{10}$ M$_\odot$
$M_{\star,2} = 10^{10}$ M$_\odot$
BH Separation (kpc)
t (Myr)
Major merger
Direct N^2
Direct N^2 + PN
$\epsilon_g = 5$ pc
Eccentricity
$t = 8.8$ Myr
$t = 13.7$ Myr
$t = 18.6$ Myr
$t = 23.5$ Myr

Juwels booster A100

----

1 GPU : 4770 sec
2 GPU : 2501 sec
4 GPU : 1721 sec
8 GPU : 1340 sec
16 GPU : 1212 sec

Speedup compare to direct run: ~10 - 16

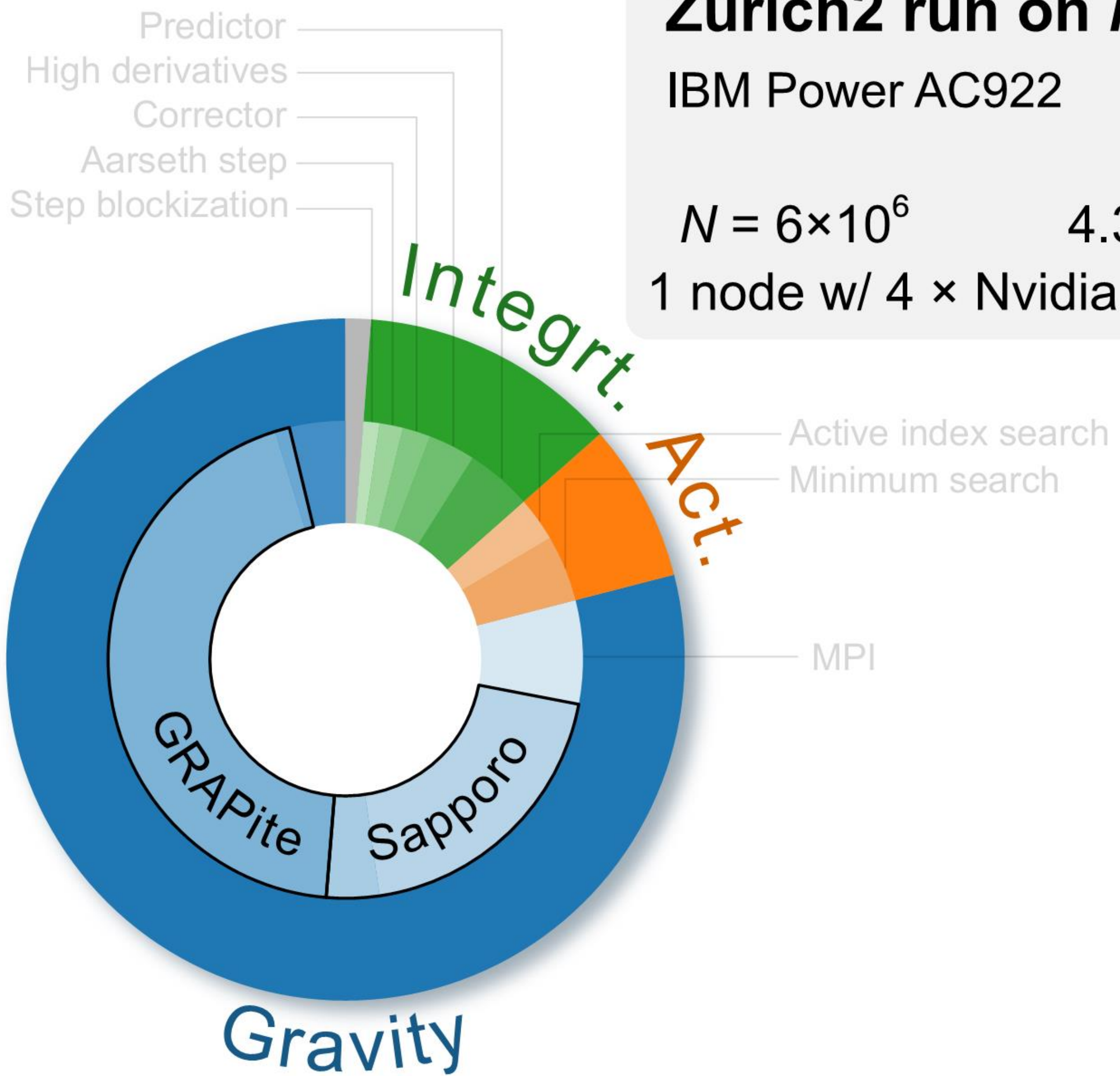

Zürich2 run on *Mist* (Toronto)

IBM Power AC922

$N = 6{\times}10^6$ 4.3% core particles

1 node w/ 4 × Nvidia Tesla V100 GPUs

79.0% Gravity
12.3% Active search
7.5% Integration